Extension of the L&M Wind Field Model to Non-Square Regions: An Improved Formulation

David G. Long, Ph.D.

29 July 1994

Extension of the L&M Wind Field Model to Non-Square Regions: An Improved Formulation

David G. Long
Brigham Young University

July 29, 1994

This report updates the L&M wind field model with an improved method for computing the curl and divergence. For completeness the entire model development and analysis is presented. A parametric descriptive model for near-surface mesoscale wind fields over the ocean, suitable for use in a new estimation-theory-based approach to estimating the wind vector field from scatterometer measurements, is developed. Two model options are considered. Finally, the ability of the resulting model to describe "realistic" near-surface mesoscale wind fields is evaluated.

In developing the model we require that the wind field model must: (1) be capable of describing near-surface mesoscale wind fields with reasonable accuracy; (2) be based only on scatterometer data (i.e., no other instrument or *in situ* data is needed); (3) be computationally tractable; and (4) lend itself to a model parameter estimation formulation.

The role of the wind field model in model-based wind field estimation is to provide a description of the wind field over the scatterometer measurement swath at a fixed instant of time and a resolution of from 25 to 50 km (corresponding to the scatterometer sampling); hence, our wind field model need only be for a sampled wind field. To simplify matters we restrict our attention to limited-area regions with a maximum spatial extent of approximately 600 km (corresponding to the maximum scatterometer swath width [10, 11]) in any direction. The scatterometer swath will be segmented in the along-track direction to appropriately sized regions.

1 Wind Field Model Assumptions

Denote the near-surface horizontal wind field of interest (e.g., the neutral stability wind at 19.5 m) by $\mathbf{U} = (u, v)^T$. We are interested in a mathematical model that provides a reasonably accurate description of $\mathbf{U}$ over a (limited-area) region $\mathcal{L}$. The vorticity ζ and divergence δ of $\mathbf{U}$ are defined, as

$$\zeta = \mathbf{k} \cdot \nabla \times \mathbf{U} \tag{1}$$
$$\delta = \nabla \cdot \mathbf{U}. \tag{2}$$

Using the Helmholtz Theorem, $\mathbf{U}$ may be defined by a streamfunction ψ and velocity potential χ, according to

$$\mathbf{U} = \mathbf{k} \times \nabla\psi + \nabla\chi \tag{3}$$

where $\mathbf{k} \times \nabla\psi$ is a nondivergent vector field and $\nabla\chi$ is a curl-free vector field [2].

Taking the divergence and curl, respectively, of Eq. (3) we obtain Poisson equations for ψ and χ [14],

$$\nabla^2\psi = \zeta \tag{4}$$
$$\nabla^2\chi = \delta \tag{5}$$

These equations appear in the classic problems of partitioning a given wind field into its rotational and non-divergent components and reconstructing a wind field from specified vorticity and divergence [2, 7, 14, 22]. For this latter problem, Lynch [14] argues that the reconstruction is not unique over a limited domain; an arbitrary harmonic function may be added to χ, provided ψ is also altered, to produce the same wind field (see [15]). From this he concludes that the boundary values of χ may be set arbitrarily. He shows that setting the boundary values of χ to zero minimizes the divergent component of the kinetic energy. Choosing $\chi = 0$ on the boundary ensures a unique reconstruction of the wind field.

Following this line of reasoning, our *first* modeling assumption is to assume that $\chi = 0$ on the boundary of $\mathcal{L}$ which corresponds to assuming that the wind field has a minimum of divergent kinetic energy. Assuming that $\chi = 0$ on the boundary, Eqs. (4) and (5), the vorticity and divergence fields, and the boundary conditions for ψ, are sufficient for describing the wind vector field.

To obtain simple boundary conditions we make a *second* major modeling assumption by attributing ψ to geostrophic motion. This second assumption is that the streamfunction ψ is proportional to the geostrophic pressure field p, i.e.,

$$\psi = \frac{1}{\rho_s f} p \tag{6}$$

where ρ_s is the density and f is the Coriolis parameter. This represents a departure from Lynch's [14] direct method for reconstructing a wind field from the normal velocity component along the boundary and the vorticity and divergence fields. Our approach allows further simplification of the model at a later step.

Note that in a strictly geostrophic formulation, the wind field would be non-divergent and χ would be identically zero. Mesoscale winds, however, may exhibit non-zero divergence; hence, we adopt a more general formulation in which χ is not set to zero. Instead, χ is attributed to the *ageostrophic* component of the wind. This generalization allows us to apply the model to mesoscale wind fields which depart from strict geostrophy. Inclusion of the ageostrophic flow permits the model to span a wider space in describing the wind field. Note that in applying the wind field model, ψ and χ will be determined from the observed wind field.

By making our second modeling assumption, we are able to specify the boundary values for Eqs. (4) and (5) in terms of the geostrophic pressure field. This avoids the difficulties

2

of using velocity boundary conditions, which may yield an overdetermined system (see the discussion in [14]).

Our *third* modeling assumption is that, over the region of interest, $\rho_s f$ is essentially constant (i.e., an f-plane approximation); we do this to simplify the mathematics. We can then normalize the pressure field by $\rho_s f$ so that $\psi = p$ (recognizing the limitation at the equator). Doing this, Eq. (3) can be written in component form, as

$$u = -\frac{\partial p}{\partial y} + \frac{\partial \chi}{\partial x} \tag{7}$$

$$v = \frac{\partial p}{\partial x} + \frac{\partial \chi}{\partial y} \tag{8}$$

These two equations, along with Eqs. (4) (in which $\psi = p$) and (5) form the basis of our wind field model.

To complete the wind-field model, descriptions of the vorticity and divergence fields are needed. Our *fourth* and final modeling assumption is that the vorticity and divergence fields are continuous, relatively smooth, and vary slowly over the region of interest, $\mathcal{L}$; hence, the vorticity and divergence fields can be parameterized using only a small number of unknowns. This is consistent with some of the limited data available [4, 5, 16, 19, 20, 21, 23],

$$\zeta(x,y) \triangleq \sum_{m=0}^{M_c} \sum_{\substack{n=0 \\ m+n \leq \max(M_c, N_c)}}^{N_c} c_{m,n} x^m y^n \tag{9}$$

$$\delta(x,y) \triangleq \sum_{m=0}^{M_d} \sum_{\substack{n=0 \\ m+n \leq \max(M_d, N_d)}}^{N_d} d_{m,n} x^m y^n \tag{10}$$

where M_c, N_c, M_d and N_d are the model orders and $c_{m,n}$ and $d_{m,n}$ are vorticity and divergence coefficients. Note that the coefficients of the polynomials will be derived from the observed wind fields.

The model orders can be selected arbitrarily (depending on the desired accuracy of the model); however, we have found, based on the results presented below, that $M_c = N_c = M_d = N_d = 2$ is adequate for wind estimation.

2 Model Development

To further develop our simple wind field model, for the purposes of wind field estimation from scatterometer measurements, we discretize Eqs. (4), (5), and (7) - (10), on an $M \times N$ equally-spaced grid with spacing h over the region $\mathcal{L}$. For our purposes the value of h is selected to correspond to the 25-50 km sampling resolution of the wind scatterometer. The swath is segmented into abutting along-track regions (see Figure 1). In the case of NSCAT, $N = 24$ and $h = 25$ km will cover the entire left or right swath width [10, 11]. For SASS $h = 50$ km. By further segmenting the swath into adjacent cross-track regions N may be chosen to be less than 24. In this case, the $Mh \times Nh$ dimensions of the region $\mathcal{L}$ are
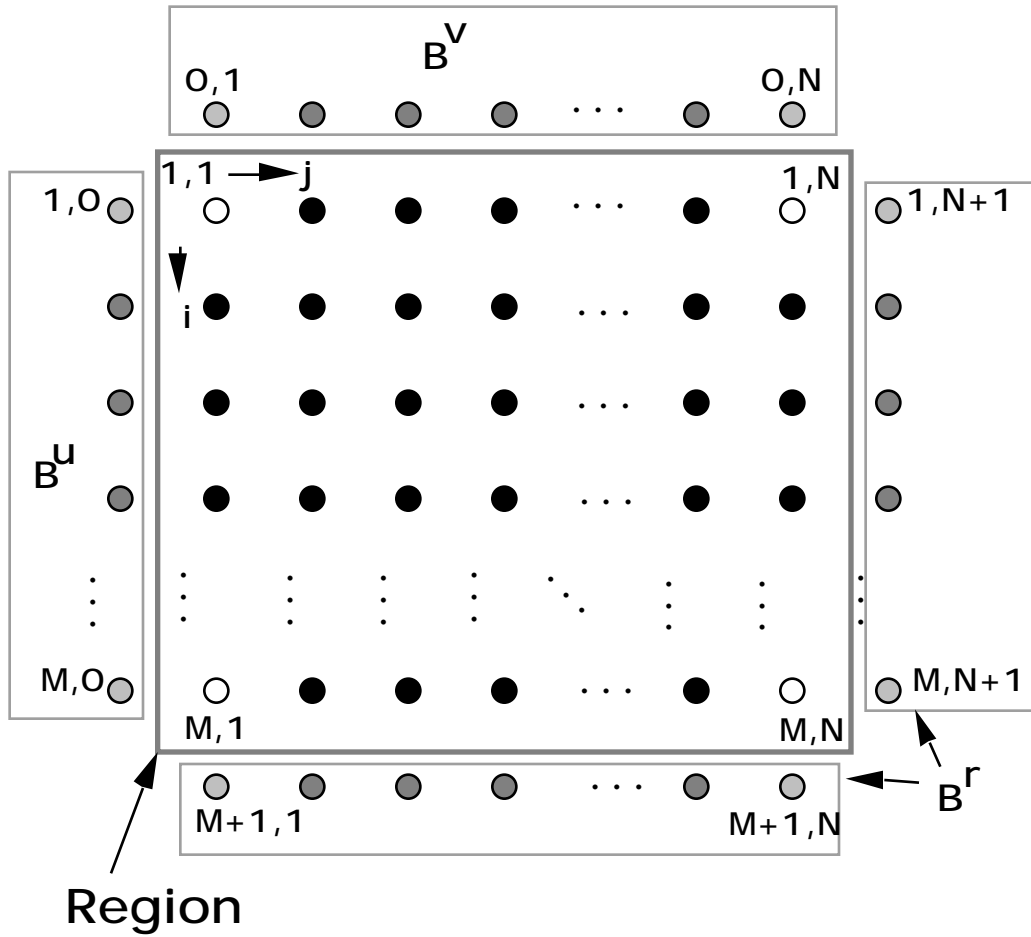
Figure 1: A diagram showing the region sample grid with boundary conditions and coordinate system. The dark sample points and open circles are the locations of the samples in the region of interest. The grey samples points indicate the locations of the boundary conditions for the pressure field (see text).

reduced. We have found that choosing $M = N = 8$ or 12 provides a good tradeoff between the number of unknowns in the model and the model's accuracy.

The discretization of Eqs. (4), (5), and (7) - (10) is stable and will converge assuming that the boundary conditions of the pressure fields are bounded and have bounded higher-order derivatives [17, 18].

We will show below that a simple linear equation can be used to relate the wind vector field at the sample points to the boundary conditions for ψ (i.e., the geostrophic pressure field along the region boundary) and the parameters of the vorticity and divergence field models.

To further develop the model we must discretize the partial differential equations [17]. For the first partial derivative we employ first-order differences. We can apply either a forward step or an backward step difference approximation. We will find it convenient to use both when computing the wind components from the pressure and velocity potential fields. A backward difference will be used on the pressure field while a forward difference will be used with the velocity potential field. This enables a first-order backward difference approximation to be used in computing the curl and divergence of the wind field.

Applying the first-order difference approximations,

$$\frac{\partial}{\partial x} a(x)\,|_{x\,=\,ih} \;\approx\; \frac{1}{h}[a(x_i) - a(x_{i-1})] \quad \text{backward difference} \tag{11}$$

$$\frac{\partial}{\partial x} a(x)\,|_{x\,=\,ih} \;\approx\; \frac{1}{h}[a(x_{i+1}) - a(x_i)] \quad \text{forward difference} \tag{12}$$

$$\frac{\partial^2}{\partial x^2} a(x)\,|_{x\,=\,ih} \;\approx\; \frac{1}{h^2}[a(x_{i+1}) - 2a(x_i) + a(x_{i-1})] \tag{13}$$

to Eqs. (4), (5), (7), and (8) and scaling by the discretization interval h, we obtain the following finite-difference equation (FDE) system,

$$
\begin{align}
u(x_i, y_j) &= -[p(x_i, y_j) - p(x_i, y_{j-1})] + [\chi(x_{i+1}, y_j) - \chi(x_i, y_j)] \tag{14} \\
v(x_i, y_j) &= [p(x_i, y_j) - p(x_{i-1}, y_j)] + [\chi(x_i, y_{j+1}) - \chi(x_i, y_j)] \tag{15} \\
\zeta(x_i, y_j) &= p(x_{i+1}, y_j) + p(x_i, y_{j+1}) \\
&\quad + p(x_{i-1}, y_j) + p(x_i, y_{j-1}) - 4p(x_i, y_j) \tag{16} \\
\delta(x_i, y_j) &= \chi(x_{i+1}, y_j) + \chi(x_i, y_{j+1}) + \chi(x_{i-1}, y_j) \\
&\quad + \chi(x_i, y_{j-1}) - 4\chi(x_i, y_j) \tag{17}
\end{align}
$$

where $i = 1, \ldots, M$ and $j = 1, \ldots, N$, and where, for convenience, $\zeta(x_i, y_i)$ and $\delta(x_i, y_i)$ have been scaled by an additional factor of h. The boundary conditions for the p field are the geostrophic pressure field $p(x_0, y_j)$ and $p(x_{M+1}, y_j)$ for $j = 1, \ldots, N$ and $p(x_i, y_0)$ and $p(x_i, y_{N+1})$ for $i = 1, \ldots, M$ (refer to Fig. 1). The boundary conditions of the χ field are assumed to be zero.

For notational simplicity we write the discretized streamfunction $p(x_i, y_j)$ as $p_{i,j}$, where $x_i = ih$ and $y_j = jh$. A similar notation will be used for the velocity, vorticity, divergence, and potential velocity fields.

Collecting the finite-difference equations for the streamfunction and potential velocity fields at each point of the square lattice covering $\mathcal{L}$, Eqs. (16) and (17) can be written as

two matrix equations, i.e.,

$$Q_M P + P Q_N = \frac{1}{4}B + \frac{1}{4}C \tag{18}$$

$$Q_M S + S Q_N = \frac{1}{4}D \tag{19}$$

where P, S, B, C, and D are $M \times N$ matrices with elements $p_{i,j}$, $\chi_{i,j}$, $b_{i,j}$, $\zeta_{i,j}$ and $\delta_{i,j}$, respectively; Q_M and Q_N are $M \times M$ and $N \times N$ dimensional, tridiagonal, symmetric, Toeplitz matricies. Q_M and Q_N have similar structure with elements $q_{i,j}$, where,

$$q_{i,j} = \begin{cases} \frac{1}{2}, & \text{if } i = j \\ -\frac{1}{4}, & \text{if } |i - j| = 1 \\ 0, & \text{otherwise.} \end{cases} \tag{20}$$

Note that $Q_M = Q_M^T$ and that $Q_N = Q_N^T$. B is a matrix containing only the p field boundary values (the geostrophic pressure field p along the boundary), i.e., the elements $b_{i,j}$ of B are,

$$b_{i,j} = \begin{cases} p_{i,0} & \text{if } 2 \leq i \leq M - 1 \text{ and } j = 1 \\ p_{i,N+1} & \text{if } 2 \leq i \leq M - 1 \text{ and } j = N \\ p_{0,j} & \text{if } i = 1 \text{ and } 2 \leq j \leq N - 1 \\ p_{M+1,j} & \text{if } i = M \text{ and for } 2 \leq j \leq N - 1 \\ p_{1,0} + p_{0,1} & \text{if } i = 1 \text{ and } j = 1 \\ p_{0,N} + p_{1,N+1} & \text{if } i = 1 \text{ and } j = N \\ p_{M,0} + p_{M+1,1} & \text{if } i = M \text{ and } j = 1 \\ p_{M,N+1} + p_{M+1,N} & \text{if } i = M \text{ and } j = N \\ 0 & \text{otherwise.} \end{cases} \tag{21}$$

For clarity, Q_M and Q_N and B are,

$$Q_M = \frac{1}{4} \begin{bmatrix} 2 & -1 & 0 & \dots & 0 \\ -1 & 2 & -1 & \ddots & \vdots \\ 0 & -1 & 2 & \ddots & 0 \\ \vdots & \ddots & \ddots & \ddots & -1 \\ 0 & \dots & 0 & -1 & 2 \end{bmatrix} \quad (M \times M), \tag{22}$$

$$Q_N = \frac{1}{4} \begin{bmatrix} 2 & -1 & 0 & \dots & 0 \\ -1 & 2 & -1 & \ddots & \vdots \\ 0 & -1 & 2 & \ddots & 0 \\ \vdots & \ddots & \ddots & \ddots & -1 \\ 0 & \dots & 0 & -1 & 2 \end{bmatrix} \quad (N \times N), \tag{23}$$

and

$$B = \begin{bmatrix} p_{0,1} + p_{1,0} & p_{0,2} & \cdots & p_{0,N-1} & p_{0,N} + p_{1,N+1} \\ p_{2,0} & 0 & \cdots & 0 & p_{2,N+1} \\ \vdots & \vdots & \ddots & \vdots & \vdots \\ p_{M-1,0} & 0 & \cdots & 0 & p_{M-1,N+1} \\ p_{M,0} + p_{M+1,1} & p_{M+1,2} & \cdots & p_{M+1,N-1} & p_{M,N+1} + p_{M+1,N} \end{bmatrix}. \tag{24}$$

We will see that the solution for the p field can be written as the sum of two independent fields; one which is solely a function of the boundary conditions for p and one which is solely a function of the ζ field. Given that the boundary conditions for the χ field are zero, the solution for the χ field depends only on the δ field.

For later convenience we decompose B into 3 $M \times N$ matrices,

$$B = B^v + B^u + B^r \tag{25}$$

where the elements of each matrix are,

$$b_{i,j}^u = \begin{cases} p_{i,0} & \text{if } j = 1, \ i = 1, \ldots, M \\ 0 & \text{otherwise} \end{cases} \tag{26}$$

$$b_{i,j}^v = \begin{cases} p_{0,j} & \text{if } i = 1, \ j = 1, \ldots, N \\ 0 & \text{otherwise} \end{cases} \tag{27}$$

$$b_{i,j}^r = \begin{cases} p_{i,N+1} & \text{if } 1 \le i \le M - 1 \text{ and } j = N \\ p_{M+1,j} & \text{if } i = M \text{ and for } 1 \le j \le N - 1 \\ p_{M,N+1} + p_{M+1,N} & \text{if } i = M \text{ and } j = N \\ 0 & \text{otherwise} \end{cases} \tag{28}$$

For clarity,

$$B^u = \begin{bmatrix} p_{1,0} & 0 & \cdots & 0 \\ \vdots & \vdots & \ddots & \vdots \\ p_{M,0} & 0 & \cdots & 0 \end{bmatrix}, \tag{29}$$

$$B^v = \begin{bmatrix} p_{0,1} & \cdots & p_{0,N} \\ 0 & \cdots & 0 \\ \vdots & \ddots & \vdots \\ 0 & \cdots & 0 \end{bmatrix}, \tag{30}$$

and

$$B^r = \begin{bmatrix} 0 & \cdots & 0 & p_{1,N+1} \\ \vdots & \ddots & \vdots & \vdots \\ 0 & \cdots & 0 & p_{N-1,N+1} \\ p_{M+1,1} & \cdots & p_{M+1,N-1} & p_{M,N+1} + p_{M+1,N} \end{bmatrix}. \tag{31}$$

Using an overbar to denote an $MN \times 1$ vector of lexicographic-ordered (row order) elements of an $M \times N$ matrix, Eqs. (18) and (19) can be reexpressed, as

$$K\overline{P} = \frac{1}{4}\overline{B} + \frac{1}{4}\overline{C} \tag{32}$$

$$K\overline{S} = \frac{1}{4}\overline{D} \tag{33}$$

where K is an $MN \times MN$ Toeplitz matrix defined, as

$$K \stackrel{\triangle}{=} I_M \otimes Q_N + Q_M \otimes I_N \qquad (34)$$

where $\otimes$ is the Kronecker-product [3, 8] and I_M and I_N are $M \times M$ and $N \times N$ dimensional identity matrices, respectively. It can be shown that K is invertible and has a simple closed form (see Appendix).

Since K is invertible, Eqs. (32) and (33) have the unique solutions,

$$\overline{P} \;=\; \frac{1}{4} K^{-1}[\overline{B} + \overline{C}] \qquad (35)$$

$$=\; \frac{1}{4} K^{-1}(\overline{B}^u + \overline{B}^v + \overline{B}^r) + \frac{1}{4} K^{-1}\overline{C} \qquad (36)$$

$$\overline{S} \;=\; \frac{1}{4} K^{-1}\overline{D} \qquad (37)$$

Starting with the first two equations of the FDE system, (14) and (15), reexpressed as

$$u_{i,j} \;=\; -(\psi_{i,j} - \psi_{i,j-1}) + (\chi_{i+1,j} - \chi_{i,j}) \qquad (38)$$

$$v_{i,j} \;=\; (\psi_{i,j} - \psi_{i-1,j}) + (\chi_{i,j+1} - \chi_{i,j}), \qquad (39)$$

where $i = 1, \dots, M$ and $j = 1, \dots, N$, we can relate the p and χ fields to the velocity field. To write Eqs. (38) and (39) in matrix form, let U and V be $M \times N$ matrices with elements $u_{i,j}$ and $v_{i,j}$, respectively. These equations can then be written, as

$$U \;=\; [P(D_N^s - I_N)^T + B^u] - (I_M - D_M^s)^T S \qquad (40)$$

$$V \;=\; [(I_M - D_M^s)P - B^v] + S(D_N^s - I_N)^T \qquad (41)$$

where D_M^s and D_N^s are an $M \times M$ and $N \times N$, respectively, matrices which have unity sub-diagonal and are zero everywhere else, i.e.,

$$(D_M^s)_{i,j} = (D_N^s)_{i,j} = \begin{cases} 1, & \text{if } j = i - 1 \\ 0, & \text{else} \end{cases} \qquad (42)$$

For clarity,

$$D_M^s = \begin{bmatrix} 0 & \dots & & \dots & 0 \\ 1 & 0 & \ddots & & \vdots \\ 0 & \ddots & \ddots & \ddots & \\ \vdots & \ddots & \ddots & \ddots & \vdots \\ 0 & \dots & 0 & 1 & 0 \end{bmatrix} \quad (M \times M). \qquad (43)$$

Using lexicographic-ordered vectors, Eqs. (40) and (41) can be written, as

$$\overline{U} \;=\; [G\overline{P} + \overline{B}^u] - H_T \overline{S} \qquad (44)$$

$$\overline{V} \;=\; [H\overline{P} - \overline{B}^v] + G_T \overline{S} \qquad (45)$$

8

where the $MN \times MN$ matrices G, H, G_T, H_T are defined, as

$$G \triangleq I_M \otimes [D_N^s - I_N] \tag{46}$$

$$H \triangleq [I_M - D_M^s] \otimes I_N \tag{47}$$

$$G_T \triangleq I_M \otimes [D_N^s - I_N]^T \tag{48}$$

$$H_T \triangleq [I_M - D_M^s]^T \otimes I_N. \tag{49}$$

By using the properties of the Kronecker product and the definition of D_N^s it can be shown that G is the block Jordan-form matrix,

$$G = \begin{bmatrix} D_N^s - I_N & 0 & \cdots & 0 \\ 0 & D_N^s - I_N & \ddots & \vdots \\ \vdots & \ddots & \ddots & 0 \\ 0 & \cdots & 0 & D_N^s - I_N \end{bmatrix}. \tag{50}$$

H is a block tridiagonal matrix,

$$H = \begin{bmatrix} I_N & 0 & 0 & \cdots & 0 \\ -I_N & I_N & 0 & \cdots & 0 \\ 0 & -I_N & I_N & \ddots & \vdots \\ \vdots & \ddots & \ddots & \ddots & 0 \\ 0 & \cdots & 0 & -I_N & I_N \end{bmatrix} \tag{51}$$

Similarly,

$$G_T = \begin{bmatrix} D_N^{sT} - I_N & 0 & \cdots & 0 \\ 0 & D_N^{sT} - I_N & \ddots & \vdots \\ \vdots & \ddots & \ddots & 0 \\ 0 & \cdots & 0 & D_N^{sT} - I_N \end{bmatrix}. \tag{52}$$

$$H_T = \begin{bmatrix} I_N & -I_N & 0 & \cdots & 0 \\ 0 & I_N & -I_N & \cdots & 0 \\ 0 & 0 & I_N & \ddots & \vdots \\ \vdots & \ddots & \ddots & \ddots & -I_N \\ 0 & \cdots & 0 & 0 & I_N \end{bmatrix} \tag{53}$$

G, H, G_T, and H_T are full rank and invertible.

Note that $\overline{B}^u$ and $\overline{B}^v$ are MN element vectors with a maximum of M and N non-zero elements, respectively, whereas $\overline{B}^r$ is an MN element vector with a maximum of $M+N-1$ non-zero elements. Consequently, there are a maximum of $2M+2N-1$ non-zero parameters in the $\overline{B}$ vector.

We note that the wind velocity is proportional to the partial derivatives (or, in this formulation, first-order differences) of the p and χ fields. An arbitrary constant can be

added or subtracted from the p and χ fields without affecting the results; hence, a constant can be added to or subtracted from the boundary condition vectors without affecting the results. Since this additive constant is arbitrary and is unimportant, we can normalize the boundary condition vectors $\overline{B}^u$, $\overline{B}^v$, and $\overline{B}^r$ so that the first element of $\overline{B}^u$, $p_{0,1}$, is zero. This effectively eliminates one non-zero parameter, reducing the number of non-zero parameters in $\overline{B}^u$, $\overline{B}^v$, and $\overline{B}^r$ from $2M + 2N - 1$ to $2M + 2N - 2$.

With this normalization accomplished, $\overline{B}^u$ and $\overline{B}^v$ will be linearly independent since they have no corresponding non-zero elements. With the exception of the $(n_1 = N)^{th}$ element, where

$$\overline{B}^v_{n_1} = p_{0,N} \tag{54}$$

and

$$\overline{B}^r_{n_1} = p_{1,N+1}, \tag{55}$$

the vectors $\overline{B}^v$ and $\overline{B}^r$ have no corresponding non-zero elements. Similarly, With the exception of the $(n_2 = MN - N + 1)^{th}$ element, where

$$\overline{B}^u_{n_2} = p_{M,0} \tag{56}$$

and

$$\overline{B}^r_{n_2} = p_{M+1,1}, \tag{57}$$

the vectors $\overline{B}^u$ and $\overline{B}^r$ have no corresponding non-zero elements.

Note, also, that the last element of $\overline{B}^r$ is the sum of two boundary values, $p_{M,N+1}$ and $p_{M+1,N}$; hence, we do not need to separately identify these values and so we need only identify the sum.

Substituting Eqs. (35) and (37) into Eqs. (44) and (45) and remembering that the boundary conditions of S are zero, we obtain

$$\overline{U} = \left[\frac{1}{4} G K^{-1} (\overline{B} + \overline{C}) + \overline{B}^u \right] - \frac{1}{4} H_T K^{-1} \overline{D} \tag{58}$$

$$= \frac{1}{4} \left[G K^{-1} (\overline{B}^r + \overline{B}^v + \overline{C}) + (G K^{-1} + 4 I_{MN}) \overline{B}^u \right] - \frac{1}{4} H_T K^{-1} \overline{D} \tag{59}$$

$$\overline{V} = \left[\frac{1}{4} H K^{-1} (\overline{B} + \overline{C}) - \overline{B}^v \right] + \frac{1}{4} G_T K^{-1} \overline{D} \tag{60}$$

$$= \frac{1}{4} \left[H K^{-1} (\overline{B}^r + \overline{B}^u + \overline{C}) + (H K^{-1} - 4 I_{MN}) \overline{B}^v \right] + \frac{1}{4} G_T K^{-1} \overline{D} \tag{61}$$

where I_{MN} is the $MN \times MN$ dimensional identity matrix.

To write Eqs. (59) and (61) as a single equation, observe that they have the general form,

$$\overline{U} = {}_1 A \overline{B}^r + {}_1 A \overline{B}^v + {}_2 A \overline{B}^u + {}_1 A \overline{C} - {}_6 A \overline{D} \tag{62}$$

$$\overline{V} = {}_3 A \overline{B}^r + {}_3 A \overline{B}^u + {}_4 A \overline{B}^v + {}_3 A \overline{C} + {}_5 A \overline{D} \tag{63}$$

where the $_jA$ matrices are defined, as

$$_1A = \frac{1}{4}GK^{-1} \tag{64}$$

$$_2A = \frac{1}{4}\left[GK^{-1} + 4I_{MN}\right] \tag{65}$$

$$_3A = \frac{1}{4}HK^{-1} \tag{66}$$

$$_4A = \frac{1}{4}\left[HK^{-1} - 4I_{MN}\right] \tag{67}$$

$$_5A = \frac{1}{4}G_TK^{-1} \tag{68}$$

$$_6A = \frac{1}{4}H_TK^{-1}. \tag{69}$$

$$\tag{70}$$

Let $\overline{X}$ be a $2M + 2N - 2$ element vector of the non-zero elements of $\overline{B}^r$, $\overline{B}^u$, and $\overline{B}^v$, where the nth element, $\overline{x}_n$, of $\overline{X}$ is,

$$\overline{x}_n = \begin{cases} \overline{B}^v_{n+1} & 1 \le n < N \\ \overline{B}^u_{(n-N)M+1} & N \le n < M + N \\ \overline{B}^r_{(n-M+N+1)N} & M + N \le n < M + 2N \\ \overline{B}^r_{n-M+2N+1} & M + 2N \le n \le 2M + 2N - 2 \end{cases} \tag{71}$$

For clarity,

$$\overline{X} = \begin{bmatrix} \overline{x}_1 \\ \overline{x}_2 \\ \vdots \\ \overline{x}_{N-1} \\ \overline{x}_N \\ \overline{x}_{N+1} \\ \overline{x}_{N+2} \\ \vdots \\ \overline{x}_{M+N-1} \\ \overline{x}_{M+N} \\ \overline{x}_{M+N+1} \\ \vdots \\ \overline{x}_{M+2N-2} \\ \overline{x}_{M+2N-1} \\ \overline{x}_{M+2N} \\ \vdots \\ \overline{x}_{2M+2N-2} \end{bmatrix} = \begin{bmatrix} p_{0,2} \\ p_{0,3} \\ \vdots \\ p_{0,N} \\ p_{1,0} \\ p_{2,0} \\ p_{3,0} \\ \vdots \\ p_{M,0} \\ p_{1,N+1} \\ p_{2,N+1} \\ \vdots \\ p_{M-1,N+1} \\ p_{M,N+1} + \psi_{M+1,N} \\ p_{M+1,1} \\ \vdots \\ p_{M+1,N-1} \end{bmatrix} = \begin{bmatrix} \overline{B}^v_2 \\ \overline{B}^v_3 \\ \vdots \\ \overline{B}^v_N \\ \overline{B}^u_1 \\ \overline{B}^u_{N+1} \\ \overline{B}^u_{2N+1} \\ \vdots \\ \overline{B}^u_{MN-N+1} \\ \overline{B}^r_N \\ \overline{B}^r_{2N} \\ \vdots \\ \overline{B}^r_{MN-N} \\ \overline{B}^r_{MN} \\ \overline{B}^r_{MN-N+1} \\ \vdots \\ \overline{B}^r_{MN-1} \end{bmatrix} \tag{72}$$

11

Define the MN element vector $\overline{W}$ as the concatenation of $\overline{U}$ and $\overline{V}$, i.e.,

$$\overline{W} = \left[\begin{array}{c} \overline{U} \\ \hline \overline{V} \end{array} \right].$$

(73)

Then, the wind field model, Eqs. (62) and (63), can be expressed as the single equation,

$$\overline{W} = F\overline{X} + R^c\overline{C} + R^d\overline{D}$$

(74)

where F is a $2MN \times (2M + 2N - 2)$ matrix and R^c and R^d are $2MN \times MN$ matrices. F, R^c and R^d are composed of columns of the A matrices in Eqs. (64) through (69).

For convenience in defining F, we partition F into 4 rectangular submatrices,

$$F = \left[\begin{array}{c|c|c|c} F_1 & F_2 & F_3 & F_4 \end{array} \right]$$

(75)

where the F_i matrices are defined, as

$$F_1 \;\; = \;\; \left[\begin{array}{c|c|c|c} {}_1A_2 & {}_1A_3 & \cdots & {}_1A_N \\ \hline {}_4A_2 & {}_4A_3 & \cdots & {}_4A_N \end{array} \right]$$

(76)

$$F_2 \;\; = \;\; \left[\begin{array}{c|c|c|c} {}_2A_1 & {}_2A_{N+1} & \cdots & {}_2A_{MN-N+1} \\ \hline {}_3A_1 & {}_3A_{N+1} & \cdots & {}_3A_{MN-N+1} \end{array} \right]$$

(77)

$$F_3 \;\; = \;\; \left[\begin{array}{c|c|c|c} {}_1A_N & {}_1A_{2N} & \cdots & {}_1A_{MN} \\ \hline {}_3A_N & {}_3A_{2N} & \cdots & {}_3A_{MN} \end{array} \right]$$

(78)

$$F_4 \;\; = \;\; \left[\begin{array}{c|c|c|c} {}_1A_{MN-N+1} & {}_1A_{MN-N+2} & \cdots & {}_1A_{MN-1} \\ \hline {}_3A_{MN-N+1} & {}_3A_{MN-N+2} & \cdots & {}_3A_{MN-1} \end{array} \right]$$

(79)

where ${}_jA_i$ is the ith column of the jth A matrix in Eqs. (64) through (69). The matrices F_1 and F_4 are $2MN \times (N - 1)$ while F_2 and F_3 are $2MN \times M$. The matrix R^c is defined, as

$$R^c = \left[\begin{array}{c} {}_1A \\ \hline {}_3A \end{array} \right]$$

(80)

whereas the matrix R^d is defined, as

$$R^d = \left[\begin{array}{c} -{}_6A \\ \hline {}_5A \end{array} \right]$$

(81)

Eq. (74) provides a single matrix-vector equation relating the wind field velocity components contained in the $2MN$ element vector $\overline{W}$ to the $2M + 2N - 2$ element boundary condition vector $\overline{X}$ and the MN element vorticity and divergence field vectors $\overline{C}$ and $\overline{D}$, respectively.

Note that Eq. (74) can be expressed, as

$$\overline{W} = \overline{W}^b + \overline{W}^c + \overline{W}^d$$

(82)

12

where

$$\overline{W}^b \triangleq F\overline{X} \tag{83}$$

$$\overline{W}^c \triangleq R^c\overline{C} \tag{84}$$

$$\overline{W}^d \triangleq R^d\overline{D} \tag{85}$$

The wind field $\overline{W}$ can therefore be expressed as the sum of a field $\overline{W}^b$ which depends only on the boundary conditions in $\overline{X}$, a field $\overline{W}^c$ which depends only on the vorticity field in $\overline{C}$, and a field $\overline{W}^d$ which depends only on the divergence field in $\overline{D}$.

From our fourth modeling assumption, we assume that the vorticity and divergence fields can be parameterized (or modeled) by a small number of unknown but deterministic parameters which are the coefficients of the bivariate polynomials in Eqs. (9) and (10). Using this parameterization, the wind field model can then be formulated in terms of the boundary conditions on the p field and the parameters of the vorticity and divergence field model. For later use we define Υ^c as the transformation matrix between the parameter vector $\overline{X}^c$ and the vorticity field $\overline{C}$, i.e.,

$$\overline{C} = \Upsilon^c\overline{X}^c \tag{86}$$

where $\overline{X}^c$ contains the parameters of the vorticity field model. Υ^d and $\overline{X}^d$ are similarily defined for the divergence field, i.e.,

$$\overline{D} = \Upsilon^d\overline{X}^d. \tag{87}$$

Using this polynomial parameterization for the vorticity and divergence fields, Eq. (74) can be written, as

$$\overline{W} = F\overline{X} + R^c \sum_{m=0}^{M_c} \sum_{\substack{n=0 \\ m+n \leq \max(M_c,N_c)}}^{M_c} c_{m,n}Q_{m,n} + R^d \sum_{m=0}^{M_d} \sum_{\substack{n=0 \\ m+n \leq \max(M_d,N_d)}}^{M_d} d_{m,n}Q_{m,n} \tag{88}$$

$$= F\overline{X} + \sum_{m=0}^{M_c} \sum_{\substack{n=0 \\ m+n \leq \max(M_c,N_c)}}^{M_c} c_{m,n}R^cQ_{m,n} + \sum_{m=0}^{M_d} \sum_{\substack{n=0 \\ m+n \leq \max(M_c,N_c)}}^{M_d} d_{m,n}R^dQ_{m,n} \tag{89}$$

where the kth element ${}_kq_{m,n}$ of the MN element vector $Q_{m,n}$ is,

$$_kq_{m,n} = \lfloor k \rfloor^m + \lceil k \rceil^n \tag{90}$$

in which $\lfloor k \rfloor \triangleq int[(k-1)/N]+1$ and $\lceil k \rceil \triangleq mod(k-1,N)+1$. The constant vorticity or divergence case corresponds to $M_c = N_c = 0$ or $M_d = N_d = 0$, respectively. The case when the vorticity or divergence is assumed to be identically zero will be denoted by $M_c = N_c = -1$ or $M_d = N_d = -1$, respectively.

A simple special case occurs for $M_c = N_c = M_d = M_d = 1$; then,

$$\zeta_{i,j} = c_{0,0} + c_{1,0}i + c_{0,1}j \tag{91}$$

$$\delta_{i,j} = d_{0,0} + d_{1,0}i + d_{0,1}j \tag{92}$$

13

so that Eq. (74) can be written, as

$$\overline{W} = F\overline{X} + c_{0,0}\overline{R}^c + c_{1,0}\overline{R}_x^c + c_{0,1}\overline{R}_y^c + d_{0,0}\overline{R}^d + d_{1,0}\overline{R}_x^d + c_{0,1}\overline{R}_y^d \qquad (93)$$

where $\overline{R}^c$, $\overline{R}^d$, $\overline{R}_x^c$, $\overline{R}_y^c$, $\overline{R}_x^d$, and $\overline{R}_y^d$ are $2MN$ vectors with elements $\overline{R}_k^c$, $\overline{R}_k^d$, $\overline{R}_{x_k}^c$, $\overline{R}_{y_k}^c$, $\overline{R}_{x_k}^d$ and $\overline{R}_{y_k}^d$ defined, as

$$\overline{R}_k^c = \sum_{i=1}^{M}\sum_{j=1}^{N} r_{k,j+(i-1)N}^c \qquad (94)$$

$$\overline{R}_k^d = \sum_{i=1}^{M}\sum_{j=1}^{N} r_{k,j+(i-1)N}^d \qquad (95)$$

$$\overline{R}_{x_k}^c = \sum_{i=1}^{M} i \sum_{j=1}^{N} r_{k,j+(i-1)N}^c \qquad (96)$$

$$\overline{R}_{y_k}^c = \sum_{j=1}^{N} j \sum_{i=1}^{M} r_{k,j+(i-1)N}^c \qquad (97)$$

$$\overline{R}_{x_k}^d = \sum_{i=1}^{M} i \sum_{j=1}^{N} r_{k,j+(i-1)N}^d \qquad (98)$$

$$\overline{R}_{y_k}^d = \sum_{j=1}^{N} j \sum_{i=1}^{M} r_{k,j+(i-1)N}^d \qquad (99)$$

where $r_{k,j}^c$ and $r^d k,j$ are the elements of R^c and R^d, respectively.

To express Eq. (93) in a simple form, we define a new $2M + 2N + 4$ parameter vector $\overline{X}_r$ by augmenting $\overline{X}$ with $c_{0,0}$, $c_{1,0}$, $c_{0,1}$, $d_{0,0}$, $d_{1,0}$ and $d_{0,1}$, i.e.,

$$\overline{X}_r = \begin{bmatrix} \overline{X} \\ c_{0,0} \\ c_{1,0} \\ c_{0,1} \\ d_{0,0} \\ d_{1,0} \\ d_{0,1} \end{bmatrix} = \begin{bmatrix} \overline{X}^c \\ \overline{X}^d \end{bmatrix} \qquad (100)$$

and let the $2MN \times (2M + 2N + 4)$ matrix F_r be the matrix created by column-augmenting the matrix F with $\overline{R}$, $\overline{R}_x^c$, etc.; i.e.,

$$F_r = \begin{bmatrix} F & \overline{R}^c & \overline{R}_x^c & \overline{R}_y^c & \overline{R}^d & \overline{R}_x^d & \overline{R}_y^d \end{bmatrix}. \qquad (101)$$

Equation (93) can then be written, as

$$\overline{W} = F_r \overline{X}_r \qquad (102)$$

14

Since G, H and K are invertible, $_1A$ and $_3A$ are full rank (i.e., they have independent columns) and invertible. It is shown that the columns of F are linearly independent in the appendix; hence, F is full rank. It follows from the definitions of R^c and R^d that the columns of R^c and R^d are linearly independent. We note that $\overline{R}^c$, $\overline{R}^c$, $\overline{R}^c_x$ $\overline{R}^c_y$, $\overline{R}^d_x$ and $\overline{R}^d_y$ are linearly independent of each other (for $N > 3$) and, further, that these vectors are independent of the columns of F. It follows that the columns of F_r are linearly independent so that F_r is full rank; hence, there is a unique relationship between a given $\overline{W}$ and the parameters $\overline{X}_r$. Given $\overline{W}$, a least-squares estimate of $\overline{X}_r$ is,

$$\overline{X}_r = F_r^\dagger \overline{W} \tag{103}$$

where $F_r^\dagger$ is the generalized inverse of F_r. Since the system of equations is overdetermined, $F_r^\dagger = (F_r^T F_r)^{-1} F_r^T$.

The extension of this approach of augmenting the parameters of the vorticity and divergence field models to the boundary conditions for higher-order polynomial orders is straightforward.

3   Parameterizing the Boundary Conditions

For a given choice of M_c, N_c, M_d and N_d, the final wind field model has the form of Eq. (102); the wind field is a simple linear function of the boundary conditions for p and the parameters of the vorticity and divergence fields. This model is referred to as the normal boundary (NB) wind field model.

Early in the testing of this wind field model, it became apparent that, since the geostrophic pressure field tends to be very smooth at the mesoscale, the number of unknown boundary values can be reduced by parameterizing the geostrophic pressure field around the region's boundary. While not a required part of our wind field model, minimizing the number of unknown parameters in the model significantly reduces the CPU time required to determine the optimum model parameters, when our model is applied to wind field estimation from wind scatterometer measurements.

We note that the pressure field around the square region of interest will be continuous. Since the boundary is closed, the pressure field along the boundary will be periodic. We now parameterize the pressure p as a one-dimensional function along the boundary of the region $\mathcal{L}$. We write the pressure field around the boundary as $p(l)$, where l is related to the discretization grid indexes i and j clockwise around the boundary, according to

$$l = \begin{cases} j, & i = 0,\ 0 \leq j \leq N+1, \\ i + N + 1, & j = N+1,\ 0 < i \leq M+1, \\ 2N + M + 3 - j, & i = M+1,\ 0 \leq j \leq N+1, \\ 2M + 2N - i, & j = 0,\ 0 \leq i < M+1. \end{cases} \tag{104}$$

This formulation provides a one-to-one mapping from l to the region's boundary. Observe that l runs from 0 to $2M + 2N + 4$. For notational simplicity, we write $p(l)$ as p_l.

Since p_l is "smooth" and must be periodic (that is, $p_0 = p_{(2M+2N+4)}$), a low-order Fourier series representation is appropriate for it, i.e.,

$$p_l = s_0 + \sum_{k=1}^{M_l/2} \left[s_k^c \cos\left(\frac{kl\pi}{M+N+2}\right) + s_k^s \sin\left(\frac{kl\pi}{M+N+2}\right) \right] \tag{105}$$

where M_l is the order of the pressure boundary condition model. We have already noted that an arbitrary constant can be added to the pressure field without affecting the model formulation, so we can ignore the s_0 term. This requires that we modify the definition of F_1 slightly to incorporate the boundary value $p_{0,1}$. Let F_1' be the $2MN \times N$ rectangular matrix defined, as

$$F_1' = \left[\begin{array}{c|c|c|c} {}_1A_1 & {}_1A_2 & \dots & {}_1A_N \\ \hline {}_4A_1 & {}_4A_2 & \dots & {}_4A_N \end{array} \right] = \left[\begin{array}{c|c} {}_1A_1 & \\ & F_1 \\ {}_4A_1 & \end{array} \right]. \tag{106}$$

Let the M_l element vector $\overline{Y}$ be defined, as

$$\overline{Y} \triangleq \begin{bmatrix} s_1^c \\ s_1^s \\ s_2^c \\ s_2^s \\ \vdots \\ s_{(M_l-1)/2}^c \\ s_{(M_l-1)/2}^s \end{bmatrix} \tag{107}$$

Equations (62) and (63) can be then be written as,

$$\overline{W} = \mathcal{F}\overline{Y} + R^c C + R^d D \tag{108}$$

where $\mathcal{F}$ is a $2MN \times M_l$ rectangular matrix created from the F_j matrices and F_1'. Let $f_{i,j}$ be the $(i,j)^{th}$ element of $\mathcal{F}$ and $(F_k)_{i,j}$ be the $(i,j)^{th}$ element of the F_k matrix; then,

$$f_{i,j} = \begin{cases} \sum_{k=1}^N (F_1')_{i,k} \cos\pi[jk/(M+N+2)-1] \\ +\sum_{k=1}^N (F_2)_{i,k} \cos\pi[j(2n+2M+4-k)/(M+N+2)] \\ +\sum_{k=1}^N (F_3)_{i,k} \cos\pi[j(n+1+k)/(M+N+2)] & \text{for } j \text{ odd} \\ +\sum_{k=1}^N (F_4)_{i,k} \cos\pi[j(2N+M+3-k)/(M+N+2)] \\ \sum_{k=1}^N (F_1')_{i,k} \sin\pi[jk/(M+N+2)] \\ +\sum_{k=1}^N (F_2)_{i,k} \sin\pi[j(2-k)/(M+N+2)] \\ +\sum_{k=1}^N (F_3)_{i,k} \sin\pi[j(1+k)/(M+N+2)] & \text{for } j \text{ even.} \\ +\sum_{k=1}^N (F_4)_{i,k} \sin\pi[j(3-k)/(M+N+2)] \end{cases} \tag{109}$$

The final parameterized boundary condition (PBC) wind field model is created by augmenting $\overline{Y}$ with the parameters of the vorticity and divergence field model, as previously done for the NB model.

Alternately, we can use a slightly different boundary polynomial parameterization based on a polar representation of the boundary positions. In this alternate boundary parameterization, the the pressure field around the boundary is expressed as $p(\theta(l))$ where $\theta(l)$ is defined below. $p(\theta)$ is then,

$$p(\theta) = \sum_{k=1}^{M_l/2} \left[s_k^c \cos(k\theta/2) + s_k^s \sin(k\theta/2) \right]. \tag{110}$$

$\theta(l)$ is defined, as

$$\theta(l) = \begin{cases} \theta_N - \tan^{-1}\left\{\frac{(N+1)/2-l}{d_N}\right\} & 0 \le l \le (N+2)/2 \\ \theta_N + \tan^{-1}\left\{\frac{l-(N+1)/2}{d_N}\right\} & (N+2)/2 < l \le N+1 \\ 2\theta_N + \theta_M - \tan^{-1}\left\{\frac{(M+2)/2-l+N+1}{d_M}\right\} & N+1 < l \le (M+2)/2+N+1 \\ 2\theta_N + \theta_M + \tan^{-1}\left\{\frac{l-(M+1)/2-N-1}{d_M}\right\} & N+2+(M+2)/2 < l \le M+N+2 \\ 3\theta_N + 2\theta_M - \tan^{-1}\left\{\frac{(N+1)/2-l+N+2+M}{d_N}\right\} & M+N+2 < l \le (N+2)/2+N+M+2 \\ 3\theta_N + 2\theta_M + \tan^{-1}\left\{\frac{l-(N+1)/2-N-2-M}{d_N}\right\} & M+N+2+(N+2)/2 < l \le 2N+M+3 \\ 4\theta_N + 3\theta_M - \tan^{-1}\left\{\frac{(M+1)/2-l+2N+3+M}{d_M}\right\} & M+2N+3 < l \le (M+2)/2+2N+M+3 \\ 4\theta_N + 3\theta_M + \tan^{-1}\left\{\frac{l-(M+1)/2-2N-3-M}{d_M}\right\} & M+2N+3+(M+2)/2 < l \le 2N+2M+4 \end{cases} \tag{111}$$

where

$$r_{MN} = \frac{1}{2}\sqrt{(M+1)^2 + (N+1)^2} \tag{112}$$

$$\theta_N = \sin^{-1}\left\{\frac{(N+1)/2}{r_{MN}}\right\} \tag{113}$$

$$\theta_M = \sin^{-1}\left\{\frac{(M+1)/2}{r_{MN}}\right\} \tag{114}$$

$$d_N = r_{MN}\cos(\theta_N) \tag{115}$$

$$d_M = r_{MN}\cos(\theta_M). \tag{116}$$

This approach to parameterizing the boundary conditions insures that the coefficients of the boundary polynomial correspond to orthongonal polynomil components.

4 Computing the Curl and Divergence from the Wind

One of the reasons for adopting separate difference approximations of the pressure and velocity potential functions is to simplify the computation of the curl and divergence from the wind field. For convenience Eqs. (14) - (17) are repeated here in short-hand notation,

$$u_{i,j} = -[p_{i,j} - p_{i,j-1}] + [\chi_{i+1,j} - \chi_{i,j}] \tag{117}$$

$$v_{i,j} = [p_{i,j} - p_{i-1,j}] + [\chi_{i,j+1} - \chi_{i,j})] \tag{118}$$

$$\zeta_{i,j} = p_{i+1,j} + p_{i,j+1} + p_{i-1,j} + p_{i,j-1} - 4p_{i,j} \tag{119}$$

$$\delta_{i,j} = \chi_{i+1,j} + \chi_{i,j+1} + \chi_{i-1,j} + \chi_{i,j-1} - 4\chi_{i,j}. \tag{120}$$

The divergence of the vector wind $\mathbf{U} = (u, v)^t$ is defined as,

$$
\begin{aligned}
\text{Div}\{\mathbf{U}\} &\triangleq \frac{\partial}{\partial x} U_x + \frac{\partial}{\partial y} U_y \\
&= \frac{\partial}{\partial x} u + \frac{\partial}{\partial y} v
\end{aligned}
\tag{121}
$$

while the vorticity is defined as,

$$
\begin{aligned}
\text{Vor}\{\mathbf{U}\} &\triangleq -\frac{\partial}{\partial y} V_x + \frac{\partial}{\partial x} V_y \\
&= -\frac{\partial}{\partial y} u + \frac{\partial}{\partial x} v.
\end{aligned}
\tag{122}
$$

The partial derivatives can be approximated by first-order differences. By using a backward difference for the divergence equation and a forward difference for the vorticity equation, we can recover the p and χ fields. The first-order difference equations are,

$$
\begin{aligned}
\text{Div}\{\mathbf{U}_{i,j}\} &\approx [u_{i,j} - u_{i-1,j}] + [v_{i,j} - v_{i,j-1}] \tag{123} \\
\text{Vor}\{\mathbf{U}_{i,j}\} &\approx -[u_{i,j+1} - u_{i,j}] + [v_{i+1,j} - v_{i,j}]. \tag{124}
\end{aligned}
$$

Substituting Eqs. (117) and (118) we obtain,

$$
\begin{aligned}
\text{Div}\{\mathbf{U}_{i,j}\} &\approx [u_{i,j} - u_{i-1,j}] + [v_{i,j} - v_{i,j-1}] \\
&= -[p_{i,j} - p_{i,j-1}] + [p_{i-1,j} - p_{i-1,j-1}] + [p_{i,j} - p_{i-1,j}] - [p_{i,j-1} - p_{i-1,j-1}] \\
&\quad + [\chi_{i+1,j} - \chi_{i,j}] - [\chi_{i+1,j-1} - \chi_{i,j-1}] + [\chi_{i,j+1} - \chi_{i,j})] - [\chi_{i,j} - \chi_{i,j-1})] \\
&= -4\chi_{i,j} + \chi_{i+1,j} + \chi_{i-1,j} + \chi_{i,j+1} + \chi_{i,j+1} \\
&= \delta_{i,j} \tag{125} \\
\text{Vor}\{\mathbf{U}_{i,j}\} &\approx -[u_{i,j+1} - u_{i,j}] + [v_{i+1,j} - v_{i,j}] \\
&= -\{-[p_{i,j+1} - p_{i,j}] + [p_{i,j} - p_{i,j-1}] + [p_{i+1,j} - p_{i,j}] - [p_{i,j} - p_{i-1,j}]\} \\
&\quad + [\chi_{i+1,j+1} - \chi_{i,j+1}] - [\chi_{i+1,j} - \chi_{i,j}] + [\chi_{i+1,j+1} - \chi_{i+1,j})] - [\chi_{i,j+1} - \chi_{i,j})] \\
&= -4p_{i,j} + p_{i+1,j} + p_{i-1,j} + p_{i,j+1} + p_{i,j+1} \\
&= \zeta_{i,j} \tag{126}
\end{aligned}
$$

Thus, ζ and δ can be directly recovered from u and v.

5 Evaluating the Wind Field Model

Both the NB and PBC wind field model options have the general form,

$$
\overline{W} = F\overline{X}
\tag{127}
$$

where $\overline{W}$ contains the components of the sampled wind field over the region $\mathcal{L}$, F is a known constant matrix, and $\overline{X}$ is the model parameter vector. We now consider how well these

18

Table 1: RMS difference between the true wind field in Fig. 2 and the field in Fig. 3.

Normalized Vector	Direction (deg)	Normalized Speed
0.09	4.29	0.06

models can represent realistic wind fields for different orders of the vorticity and divergence field models and field size N.

To evaluate the modeling error: (1) a least-squares fit of the model parameters to a real wind field was obtained; (2) the resulting "model" wind field was computed from the model parameters; and, (3) the root-mean-square (RMS) difference between the true field and the model field was computed.

The sampled "true" wind field over $\mathcal{L}$ is denoted by $\overline{W}_t$. The least-squares fit $\overline{X}$ of the model parameters to $\overline{W}_t$ is

$$\overline{X} = F^{\dagger}\overline{W}_t \tag{128}$$

where $F^{\dagger} = (F^T F)^{-1} F^T$ is the pseudo-inverse of F [9]. The wind field computed from the model parameter vector, denoted $\overline{W}$, is

$$\overline{W} = F\overline{X}. \tag{129}$$

The vector error between $\overline{W}_t$ and $\overline{W}$ is then,

$$\overline{W}_t - \overline{W} = (I - FF^{\dagger})\overline{W}_t = (I - F(F^T F)^{-1} F^T)\overline{W}_t. \tag{130}$$

To illustrate the model performance, consider Figs. 2 and 3. A simulated (described below) mesoscale wind field, sampled at 25 km with $M = N = 12$, is shown in Fig. 2. A vector length equal to the distance between samples corresponds to a wind speed of 15 m/s. The model parameter vector $\overline{X}$ was computed using Eq. (128). The model wind field $\overline{W}$ was then computed using Eq. (129) and is plotted in Fig. 3. For this example, the NB model was used with $M_c = N_c = M_d = N_d = 2$. The RMS differences between $\overline{W}_t$ and $\overline{W}$ are tabulated in Table 2[1]. In this and succeeding tables, the RMS vector error is defined as the square root of the mean squared magnitude of the vector difference between the true field and the estimated field. The value shown is normalized by the RMS vector magnitude of the true wind field. Similarly, the RMS wind speed error has been normalized by the RMS wind speed of the true wind field. Note the close agreement between the true and model wind fields.

To evaluate our model formulation we have used simulated mesoscale wind fields, since little conventional mesoscale wind field data over the ocean is available. A detailed description of how these fields were created is given in the appendix. A summary is provided here. The test wind fields were generated by state-of-the-art numerical weather prediction

---

[1]Note that this and later tables have NOT been updated to the new formulation with both forward and backward differences. However, the results are expected to be the same

Figure 2: An example of a wind field uniformly sampled with $h = 50$ km over a 600×600 km region. A vector length equal to the sample spacing corresponds to 15 m/s.

Figure 3: The "model" wind field resulting from fitting the NB model with $M_c = N_c = M_d = N_d = 4$ and $M = N = 12$ to the wind field shown in Fig. 2. Plotting conventions and scale are the same as in Fig. 2.

models at 1.875 deg resolution. The surface wind fields were interpolated to 10 km and non-divergent small-scale variability with a ak^{-2} spectrum and random phase [1, 6] added. For a given 2000×2000 km region, the value of a was selected to be consistent with the spectrum within the region [6]. The wind fields were selected to span a wide range of meteorological conditions. An example of a portion of one of the test fields is shown in Fig. 4. Regions of high vorticity and non-zero divergence are readily observable. The sampling interval is 80 km with a vector length corresponding to the sampling distance equivalent to 15 m/s.

To evaluate the modeling error for a wind field model of size $M \times N$, each wind field was segmented into $M \times N$ regions. For each region segment, the model parameters were computed using the approach described above, and the model wind field was computed from the model parameters. The RMS of the error between the true and model fields was computed over all possible regions within the original true wind field. The results for various model options are described below.

As a general rule, for fixed $M = N$, as $M_c = N_c$ and $M_d = N_d$ are increased, the modeling error is reduced. For given values of M_c, N_c, M_d, and N_d, as N and M are increased, the modeling error increases. Since the number of parameters is a function of M_c, N_c, M_d, N_d, M, and N, there is room for tradeoff between the number of model parameters and the accuracy of the wind field model

5.1   NB Model Error

Let us first consider the performance of the NB model. For the NB model the number of unknowns, N_u, in each $M \times N$ region segment is related to M, N, M_c, N_c, M_d, and N_d by the formula,

$$N_u = 2M + 2N - 2 + g(M_c, N_c) + g(M_d, N_d) \tag{131}$$

where

$$g(M,N) = \begin{cases} 0, & M < 0 \ \& \ N < 0, \\ M + 1, & N < 0 \ \& \ M \geq 0, \\ N + 1, & M < 0 \ \& \ N \geq 0, \\ (\max(M,N) + 1)(\min(M,N) + 1) - \\ (\max(M,N) - \min(M,N) + 1)(\max(M,N) - & \text{else.} \\ \min(M,N) + 2) \end{cases} \tag{132}$$

$M_c = N_c = -1$ is used to denote the case when the vorticity field is identically zero. Similarly, $M_d = N_d = -1$ denotes the case when the divergence is identically zero.

Table 4.3 shows RMS modeling error versus N for polynomial vorticity and divergence models with $M_c = M_d = 2$. With the exception of a dip at $M = N = 12$, the modeling error increases as $M = N$ increases. Table 4.4 illustrates the effects of varying $M_c = N_c$ and $M_d = N_d$ for $M = N = 8$. Table 4.5 is similar to Table 4.4, but for $M = N = 12$. As $M_c = N_c$ and $M_d = N_d$ increase, the modeling error is reduced. To minimize the number of unknowns in the model, we desire to keep M_c, N_c, M_d, and N_d small.

Figure 4: An example of the mesoscale wind fields used in evaluating the model accuracy. The field was uniformly sampled with $h = 80$ km. A vector length equal to the sample spacing corresponds to 15 m/s.

Table 2: Wind-field-model error for the NB model, with $M_c = N_c = M_d = N_d = 2$, as a function of $M = N$ for simulated mesoscale wind fields.

$M = N$	Number of Unknowns in $M \times N$ Region	Normalized RMS Error		
		Vector	Direction (deg)	Speed
4	20	0.043	1.490	0.023
6	28	0.081	3.180	0.046
8	36	0.085	3.758	0.050
10	44	0.105	4.993	0.065
12	54	0.085	4.378	0.053
14	66	0.083	4.582	0.054
16	74	0.157	10.007	0.105

5.2 PBC Model Error

The PBC model has the advantange of using a smaller number of unknowns than the NB model, but at the expense of a somewhat higher modeling error. For the PBC model the number of unknowns N_u in each $N \times N$ region is related to M_l, M_c and M_d by the formula,

$$N_u = 2M_l + g(M_c, N_c) + g(M_d, N_d). \tag{133}$$

Next we contrast the performance of the previous NB model results with those obtained for the PBC model. Table 4.6 illustrates the effect of varying M_l for $M = N = 8$ and $M_c = N_c = M_d = N_d = 2$. Table 4.7 presents the RMS errors for $M_l = 8$ and $M_c = N_c = M_d = N_d = 2$ versus N. Table 4.7 should be compared to Table 4.3; note that the errors are only slightly larger for the PBC case as compared to the NB case. Table 4.8 shows the effects of varying $M_c = N_c$ and $M_d = N_d$ for $M = N = 8$ and $M_l = 8$, whereas Table 4.9 presents similar results for $M + N = 12$. Table 4.8 should be compared with Table 4.5, whereas Table 4.9 should be compared with Table 4.6. Observe that for $M = N = 8$, setting $M_l = 8$ and $M_c = N_c = M_d = N_d = 1$, permits us to meet our desired model accuracy requirements. For $M + N = 12$ and $M_l = 8$, and $M_c = N_c = M_d = N_d = 2$, the desired accuracy requirements are met. Greater accuracy is achieved for larger M_l and/or larger $M_c = N_c$ and $M_d = N_d$.

Table 3: NB-model Error for $M = N = 8$, versus $M_c = N_c$ and $M_d = N_d$

Field Model		Unknowns	Normalized RMS Error		
$M_c = N_c$	$M_d = N_d$	N_u	Vector	Direction (deg)	Speed
-1	-1	30	0.191	8.309	0.115
-1	0	31	0.171	7.218	0.099
-1	1	33	0.165	7.044	0.095
-1	2	36	0.161	6.930	0.092
-1	3	40	0.154	6.626	0.089
-1	4	45	0.148	6.349	0.086
0	-1	31	0.133	6.013	0.084
0	0	32	0.102	4.652	0.063
0	1	34	0.098	4.485	0.060
0	2	37	0.096	4.326	0.059
0	3	41	0.094	4.270	0.058
0	4	46	0.093	4.213	0.057
1	-1	33	0.129	5.797	0.080
1	0	34	0.097	4.355	0.058
1	1	36	0.092	4.176	0.055
1	2	39	0.090	4.008	0.054
1	3	43	0.089	3.934	0.053
1	4	48	0.089	3.921	0.053
2	-1	36	0.124	5.604	0.076
2	0	37	0.092	4.105	0.055
2	1	39	0.087	3.915	0.052
2	2	42	0.085	3.758	0.050
2	3	46	0.085	3.711	0.050
2	4	51	0.084	3.683	0.050
3	-1	40	0.116	5.177	0.073
3	0	41	0.091	4.079	0.054
3	1	43	0.087	3.870	0.052
3	2	46	0.084	3.716	0.050
3	3	50	0.084	3.667	0.049
3	4	55	0.083	3.633	0.049
4	-1	45	0.102	4.557	0.064
4	0	46	0.084	3.783	0.051
4	1	48	0.079	3.576	0.047
4	2	51	0.077	3.410	0.045
4	3	55	0.076	3.360	0.045
4	4	60	0.075	3.310	0.044

Table 4: NB-model Error for $M = N = 12$, versus $M_c = N_c$ and $M_d = N_d$

Field Model		Unknowns	Normalized RMS Error		
$M_c = N_c$	$M_d = N_d$	N_u	Vector	Direction (deg)	Speed
-1	-1	46	0.234	11.207	0.148
-1	0	47	0.208	9.757	0.127
-1	1	49	0.199	9.304	0.120
-1	2	52	0.196	9.212	0.117
-1	3	56	0.191	8.954	0.115
-1	4	61	0.187	8.822	0.113
0	-1	47	0.163	8.028	0.108
0	0	48	0.123	6.256	0.082
0	1	50	0.111	5.725	0.074
0	2	53	0.107	5.502	0.071
0	3	57	0.105	5.445	0.069
0	4	62	0.105	5.373	0.070
1	-1	49	0.152	7.552	0.098
1	0	50	0.108	5.591	0.070
1	1	52	0.094	4.914	0.060
1	2	55	0.089	4.658	0.057
1	3	59	0.088	4.566	0.056
1	4	64	0.089	4.617	0.057
2	-1	52	0.149	7.449	0.095
2	0	53	0.104	5.397	0.067
2	1	55	0.089	4.666	0.056
2	2	58	0.085	4.378	0.053
2	3	62	0.083	4.289	0.052
2	4	67	0.083	4.277	0.052
3	-1	56	0.145	7.278	0.094
3	0	57	0.103	5.357	0.066
3	1	59	0.088	4.623	0.056
3	2	62	0.084	4.331	0.052
3	3	66	0.083	4.237	0.051
3	4	71	0.082	4.207	0.051
4	-1	61	0.139	6.999	0.091
4	0	62	0.102	5.374	0.066
4	1	64	0.087	4.580	0.056
4	2	67	0.081	4.227	0.051
4	3	71	0.082	4.263	0.052
4	4	76	0.083	4.439	0.053

Table 5: PBC-model Error for $M = N = 8$ and $M_c = N_c = M_d = N_d = 2$, versus M_l

M_l	Unknowns N_u	Normalized RMS Error		
		Vector	Direction (deg)	Speed
2	8	0.236	10.793	0.153
4	10	0.162	7.492	0.115
6	12	0.115	5.063	0.075
8	14	0.105	4.728	0.068

Table 6: PBC-model error, with $M_l = 8$ and $M_c = N_c = M_d = N_d = 2$, as a function of N for simulated mesoscale wind fields.

$M = N$	Number of Unknowns in $M \times N$ Region	Normalized RMS Error		
		Vector	Direction (deg)	Speed
8	20	0.105	4.728	0.068
10	20	0.107	5.020	0.072
12	20	0.110	5.604	0.076
14	20	0.112	5.889	0.079
16	20	0.117	6.559	0.082
18	20	0.123	7.189	0.087

Table 7: PBC-model Error for $M = N = 8$ and $M_l = 8$, versus $M_c = N_c$ and $M_d + N_d$

Field Model		Unknowns	Normalized RMS Error		
$M_c = N_c$	$M_d = N_d$	N_u	Vector	Direction (deg)	Speed
-1	-1	8	0.203	8.965	0.126
-1	0	9	0.185	7.963	0.112
-1	1	11	0.179	7.796	0.108
-1	2	14	0.175	7.611	0.106
-1	3	18	0.168	7.346	0.102
-1	4	23	0.162	7.018	0.099
0	-1	9	0.150	6.860	0.097
0	0	10	0.123	5.684	0.080
0	1	12	0.119	5.545	0.077
0	2	15	0.117	5.315	0.076
0	3	19	0.115	5.220	0.075
0	4	24	0.113	5.110	0.072
1	-1	11	0.146	6.638	0.094
1	0	12	0.118	5.424	0.076
1	1	14	0.114	5.263	0.073
1	2	17	0.111	5.021	0.072
1	3	21	0.110	4.943	0.071
1	4	26	0.108	4.849	0.069
2	-1	14	0.140	6.403	0.090
2	0	15	0.112	5.140	0.072
2	1	17	0.108	4.974	0.069
2	2	20	0.105	4.728	0.068
2	3	24	0.105	4.704	0.067
2	4	29	0.102	4.592	0.064
3	-1	18	0.133	6.033	0.087
3	0	19	0.111	5.106	0.070
3	1	21	0.106	4.960	0.067
3	2	24	0.103	4.721	0.065
3	3	28	0.103	4.693	0.064
3	4	33	0.100	4.537	0.062
4	-1	23	0.121	5.487	0.078
4	0	24	0.104	4.788	0.066
4	1	26	0.099	4.623	0.062
4	2	29	0.096	4.406	0.060
4	3	33	0.095	4.362	0.059
4	4	38	0.093	4.218	0.057

Table 8: PBC-model error for $M = N = 12$ and $M_l = 8$, versus $M_c = N_c$ and $M_d = N_d$

Field Model		Unknowns	Normalized RMS Error		
$M_c = N_c$	$M_d = N_d$	N_u	Vector	Direction (deg)	Speed
-1	-1	8	0.247	11.844	0.160
-1	0	9	0.222	10.508	0.141
-1	1	11	0.213	10.043	0.134
-1	2	14	0.210	9.875	0.131
-1	3	18	0.206	9.672	0.129
-1	4	23	0.201	9.444	0.126
0	-1	9	0.181	8.983	0.121
0	0	10	0.145	7.392	0.099
0	1	12	0.134	6.866	0.091
0	2	15	0.130	6.621	0.089
0	3	19	0.128	6.511	0.088
0	4	24	0.126	6.390	0.086
1	-1	11	0.170	8.424	0.114
1	0	12	0.132	6.719	0.089
1	1	14	0.119	6.142	0.081
1	2	17	0.115	5.876	0.079
1	3	21	0.114	5.747	0.078
1	4	26	0.111	5.627	0.076
2	-1	14	0.166	8.277	0.111
2	0	15	0.128	6.507	0.087
2	1	17	0.115	5.912	0.078
2	2	20	0.110	5.604	0.075
2	3	24	0.109	5.505	0.074
2	4	29	0.106	5.347	0.073
3	-1	18	0.163	8.146	0.109
3	0	19	0.126	6.505	0.085
3	1	21	0.113	5.902	0.076
3	2	24	0.109	5.611	0.074
3	3	28	0.108	5.508	0.073
3	4	33	0.104	5.336	0.070
4	-1	23	0.157	7.875	0.105
4	0	24	0.122	6.329	0.082
4	1	26	0.110	5.757	0.073
4	2	29	0.105	5.474	0.071
4	3	33	0.104	5.350	0.070
4	4	38	0.101	5.208	0.068

6 Conclusion

In this report the development of a model for near-surface mesoscale wind fields which is suitable for use in model-based estimation of wind fields from wind scatterometer measurements is presented. The modeling error is evaluated by means of simulation. Only a summary of the modeling error computations has been shown here.

The parameterized boundary condition model with $N = M = 8$, $M_l = 8$, and $M_c = N_c = M_d = N_d = 1$ or $M + N = 12$, $M_l = 8$, and $M_c = N_c = M_d = N_d = 2$ provides the desired model accuracy while minimizing the number of unknowns. Larger values of M_l, M_c, N_c, M_d, and N_d produce more accurate models.

Table 9: PBC-model Error for $M = N = 8$ and $M_l = 8$, versus $M_c = N_c$ and $M_d + N_d$. Circular case.

Field Model		Unknowns		Normalized RMS Error		
$M_c = N_c$	$M_d = N_d$	N_u		Vector	Direction (deg)	Speed
-1	-1	8	~ 72	0.291	13.810	0.175
0	0	10	~ 90	0.170	8.005	0.112
1	1	14	~ 126	0.145	6.903	0.099
2	2	20	~ 180	0.137	6.575	0.093
3	3	28	~ 252	0.124	6.106	0.081
4	4	38	~ 342	0.104	5.270	0.063

Detailed Derivations for the Wind Field Model

In this appendix, detailed derivations and proofs used in the derivation of the wind field model are provided. This includes a proof of the invertibility of the K matrix, the computation of K^{-1}, and a proof of the linear independence of the columns of the F matrix.

A Computation of K^{-1}

The $MN \times MN$ matrix K is defined, as

$$K = I_M \otimes Q_N + Q_M \otimes I_N \tag{134}$$

where Q_M and Q_N are $M \times M$ and $N \times N$, respectively, tridiagonal matrices with elements $q_{i,j}$, where

$$q_{i,j} = \begin{cases} \frac{1}{2}, & \text{if } i = j, \\ -\frac{1}{4}, & \text{if } |i - j| = 1, \\ 0, & \text{otherwise} \end{cases} \tag{135}$$

and I_M and I_N are $M \times M$ and $N \times N$ dimensional, respectively, identity matrices.

We will exploit the well known fact [8, 17] that the unitary sine transform matrix Ψ_M with elements $\psi_{i,j}^M$ diagonalizes Q_M, where

$$\psi_{i,j}^M = \sqrt{\frac{2}{M+1}} \sin\left(\frac{ij\pi}{M+1}\right) \tag{136}$$

and

$$\Psi_M Q_M \Psi_M^T = \Psi_M Q_M \Psi_M = \Lambda_M^q \tag{137}$$

where the off-diagonal elements of Λ_M^q are zero and the diagonal elements $\lambda_{M_{i,i}}^q \triangleq \lambda_M^q(i)$ of Λ_M^q are

$$\lambda_M^q(i) = \frac{1}{2}\left[1 - \cos\left(\frac{i\pi}{M+1}\right)\right] \quad (i = 1, \ldots, M). \tag{138}$$

Similarily, the unitary sine transform matrix Ψ_N with elements $\psi_{i,j}^N$ diagonalizes Q_N, where

$$\psi_{i,j}^N = \sqrt{\frac{2}{N+1}} \sin\left(\frac{ij\pi}{N+1}\right) \tag{139}$$

and

$$\Psi_N Q_N \Psi_N^T = \Psi_N Q_N \Psi_N = \Lambda_N^q \tag{140}$$

where the off-diagonal elements of Λ_N^q are zero and the diagonal elements $\lambda_{N_{i,i}}^q \triangleq \lambda_N^q(i)$ of Λ_N^q are

$$\lambda_N^q(i) = \frac{1}{2}\left[1 - \cos\left(\frac{i\pi}{N+1}\right)\right] \quad (i = 1, \ldots, N). \tag{141}$$

We can explictly compute the elements $q_{N_{i,j}}^{-1}$ of Q_N^{-1}, as

$$
\begin{aligned}
q_{N_{i,j}}^{-1} &= \sum_{k=1}^{N} \psi_{N_{i,k}} \psi_{N_{k,j}} / \lambda_N^q(i) \\
&= \frac{4}{N+1} \sum_{k=1}^{N} \left[\sin\left(\frac{ik\pi}{N+1}\right) \sin\left(\frac{jk\pi}{N+1}\right) \right] / \left[1 - \cos\left(\frac{k\pi}{N+1}\right) \right]] \\
&= \frac{2}{N+1} \sum_{k=1}^{N} \left[\cos\left(\frac{k(i-j)\pi}{N+1}\right) - \cos\left(\frac{k(i+j)\pi}{N+1}\right) \right] / \\
&\qquad \left[1 - \cos\left(\frac{k\pi}{N+1}\right) \right]
\end{aligned}
\tag{142}
$$

and the elements $q_{M_{i,j}}^{-1}$ of Q_M^{-1}, as

$$
\begin{aligned}
q_{M_{i,j}}^{-1} &= \sum_{k=1}^{M} \psi_{M_{i,k}} \psi_{M_{k,j}} / \lambda_M^q(i) \\
&= \frac{4}{M+1} \sum_{k=1}^{M} \left[\sin\left(\frac{ik\pi}{M+1}\right) \sin\left(\frac{jk\pi}{M+1}\right) \right] / \left[1 - \cos\left(\frac{k\pi}{M+1}\right) \right]] \\
&= \frac{2}{M+1} \sum_{k=1}^{M} \left[\cos\left(\frac{k(i-j)\pi}{M+1}\right) - \cos\left(\frac{k(i+j)\pi}{M+1}\right) \right] / \\
&\qquad \left[1 - \cos\left(\frac{k\pi}{M+1}\right) \right]
\end{aligned}
\tag{143}
$$

The Ψ_M amd Ψ_N can be used to diagonalize K. Using the elementary properties of the Kronecker product and noting that $\Psi_M^T \Psi_M = \Psi_M \Psi_M = I_M$ and $\Psi_N^T \Psi_N = \Psi_N \Psi_N = I_N$ we see that,

$$
\begin{aligned}
(\Psi_M \otimes \Psi_N) K (\Psi_M \otimes \Psi_N) &= (\Psi_M \otimes \Psi_N)(I_M \otimes Q_N + Q_M \otimes I_N)(\Psi_M \otimes \Psi_N) \\
&= (\Psi_M \otimes \Psi_N)(I_M \otimes Q_N)(\Psi_M \otimes \Psi_N) + \\
&\qquad (\Psi_M \otimes \Psi_N)(Q_M \otimes I_N)(\Psi_M \otimes \Psi_N) \\
&= (\Psi_M \otimes \Psi_M)([I_M \Psi_M] \otimes [Q_N \Psi_N]) + \\
&\qquad (\Psi_M \otimes \Psi_N)([Q_M \Psi_M] \otimes [I_N \Psi_N]) \\
&= ([\Psi_M I_M \Psi_M] \otimes [\Psi_N Q_N \Psi_N]) + ([\Psi_M Q_M \Psi_M] \otimes [\Psi_N I_N \Psi_N]) \\
&= I_M \otimes (\Psi_N Q_N \Psi_N) + (\Psi_M Q_M \Psi_M) \otimes I_N \\
&= I_M \otimes \Lambda_N^q + \Lambda_M^q \otimes I_N \\
&\triangleq \Lambda
\end{aligned}
\tag{144}
$$

Note that the matrices $I_M \otimes \Lambda_N^q$ and $\Lambda_M^q \otimes I_N$ are diagonal matrices with off-diagonal elements zero so that Λ is also diagonal. It follows from Eqs. (138) and (138) that the MN eigenvalues of Λ (which are also the eigenvalues of K) are,

$$
\lambda_{k,k} \triangleq \lambda(k) = \lambda_M^q(i) + \lambda_N^q(j) = 1 - \frac{1}{2}\cos[i\pi/(M+1)] - \frac{1}{2}\cos[j\pi/(N+1)]
\tag{145}
$$

where $i = \mathrm{mod}(k-1, N) + 1$ and $j = \mathrm{int}((k-1)/N) + 1$. Note that the eigenvalues of K are strictly positive, i.e.,

$$0 < \lambda(k) < 2 \quad \text{for all } k \tag{146}$$

With strictly positive eigenvalues, K is invertible. The eigenvalues of K^{-1} are the inverse of the eigenvalues of K, i.e.,

$$\lambda_{k,k}^{K^{-1}} \triangleq \lambda^{K^{-1}}(k) = \frac{1}{\lambda_M^q(i) + \lambda_N^q(j)} = \frac{2}{2 - \cos[i\pi/(M+1)] - \cos[j\pi/(N+1)]} \tag{147}$$

We can explictly write the elements $k_{m,n}^{-1}$ of K^{-1}, as

$$
\begin{aligned}
k_{m,n}^{-1} &= \sum_{l=1}^{MN} (\Psi_M \otimes \Psi_N)_{m,l} \lambda^{K^{-1}}(l) (\Psi_M \otimes \Psi_N)_{l,n} \\
&= \sum_{l=1}^{MN} \psi_{M\lfloor m \rfloor, \lfloor l \rfloor} \psi_{N\lceil m \rceil, \lceil l \rceil} \psi_{M\lfloor n \rfloor, \lfloor l \rfloor} \psi_{N\lceil n \rceil, \lceil l \rceil} / \lambda(l) \\
&= \frac{8}{(M+1)(N+1)} \sum_{l=1}^{MN} \sin\left(\frac{\lfloor m \rfloor \lfloor l \rfloor \pi}{M+1}\right) \sin\left(\frac{\lceil m \rceil \lceil l \rceil \pi}{N+1}\right) \cdot \\
&\qquad \sin\left(\frac{\lfloor n \rfloor \lfloor l \rfloor \pi}{M+1}\right) \sin\left(\frac{\lceil n \rceil \lceil l \rceil \pi}{N+1}\right) / \\
&\qquad \left[2 - \cos\left(\frac{i\pi}{M+1}\right) - \cos\left(\frac{j\pi}{N+1}\right)\right]
\end{aligned}
\tag{148}
$$

where $\lfloor i \rfloor \triangleq int((i-1)/N) + 1$ and $\lceil i \rceil \triangleq mod(i-1, N) + 1$.

B   Linear Independence of the Columns of F

In this section the linear independence of the columns of the F matrix is shown. For convenience in defining F, F is partitioned into 4 submatrices,

$$F = \left[\; F_1 \mid F_2 \mid F_3 \mid F_4 \;\right] \tag{149}$$

where the F_i matrices are defined, as

$$F_1 = \left[\begin{array}{c|c|c|c} {}_1A_2 & {}_1A_3 & \dots & {}_1A_N \\ \hline {}_4A_2 & {}_4A_3 & \dots & {}_4A_N \end{array}\right] \tag{150}$$

$$F_2 = \left[\begin{array}{c|c|c|c} {}_2A_1 & {}_2A_{N+1} & \dots & {}_2A_{MN-N+1} \\ \hline {}_3A_1 & {}_3A_{N+1} & \dots & {}_3A_{MN-N+1} \end{array}\right] \tag{151}$$

$$F_3 = \left[\begin{array}{c|c|c|c} {}_1A_N & {}_1A_{2N} & \dots & {}_1A_{MN} \\ \hline {}_3A_N & {}_3A_{2N} & \dots & {}_3A_{MN} \end{array}\right] \tag{152}$$

$$F_4 = \left[\begin{array}{c|c|c|c} {}_1A_{MN-N+1} & {}_1A_{MN-N+2} & \dots & {}_1A_{MN-1} \\ \hline {}_3A_{MN-N+1} & {}_3A_{MN-N+2} & \dots & {}_3A_{MN-1} \end{array}\right] \tag{153}$$

33

in which $_jA_i$ is the ith column of the $_jA$ matrix,

$$_1A = \frac{1}{4}GK^{-1} \tag{154}$$

$$_2A = \frac{1}{4}\left[GK^{-1} + 4I_{MN}\right] \tag{155}$$

$$_3A = \frac{1}{4}HK^{-1} \tag{156}$$

$$_4A = \frac{1}{4}\left[HK^{-1} - 4I_{MN}\right]. \tag{157}$$

where the $MN \times MN$ matrices G and H are defined as,

$$G \triangleq I_M \otimes [D_N^s - I_N] \tag{158}$$

$$H \triangleq [I_M - D_M^s] \otimes I_N \tag{159}$$

in which D^s is an $N \times N$ matrix which has a unity sub-diagonal and is zero everywhere else, i.e., the elements $d_{i,j}^s$ of D^s are

$$d_{i,j}^s = \begin{cases} 1, & \text{if } j = i - 1 \\ 0, & \text{else} \end{cases} \tag{160}$$

The matrices F_1 and F_4 are $2MN \times (N-1)$ while F_2 and F_3, are $2MN \times N$.

Using the properties of the Kronecker product and the definitions of D_M^s and D_N^s, it can be shown that G is the block Jordan-form matrix,

$$G = \begin{bmatrix} D_N^s - I_N & 0 & \dots & 0 \\ 0 & D_N^s - I_N & \ddots & \vdots \\ \vdots & \ddots & \ddots & 0 \\ 0 & \dots & 0 & D_N^s - I_N \end{bmatrix}. \tag{161}$$

H is a block tridiagonal matrix,

$$H = \begin{bmatrix} I_N & 0 & 0 & \dots & 0 \\ -I_N & I_N & 0 & \dots & 0 \\ 0 & -I_N & I_N & \ddots & \vdots \\ \vdots & \ddots & \ddots & \ddots & 0 \\ 0 & \dots & 0 & -I_N & I_N \end{bmatrix} \tag{162}$$

Note that both G and H are full rank and invertible. It can be readily verified that the $M \times M$ dimensional matrix T_M with elements $t_{i,j}$, where

$$t_{i,j} = \begin{cases} 1, & \text{if } j \leq i \\ 0, & \text{otherwise} \end{cases} \tag{163}$$

is the inverse of the matrix $(I_M - D_M^s)$, i.e., $(I_M - D_M^s)T_M = I_M$. Similarily, it can be readily verified that the $N \times N$ dimensional matrix T_N with elements $t_{i,j}$, where

$$t_{i,j} = \begin{cases} 1, & \text{if } j \leq i \\ 0, & \text{otherwise} \end{cases} \tag{164}$$

is the inverse of the matrix $(D_N^s - I_N)$, i.e., $(D_N^s - I_N)T_N = I_N$. Hence,

$$G^{-1} = I_M \otimes T_N \tag{165}$$
$$H^{-1} = T_M \otimes I_N. \tag{166}$$

Since G and H are invertible, it follows that $_1A = GK^{-1}$ and $_3A = HK^{-1}$ are full rank with independent columns. From their definition it is readily apparent that the columns of F_3 and F_4 are linearly independent since they are composed of different columns of $_1A$ and $_3A$. In the following section we show that $_2A = (GK^{-1} + 4I)/4$ and $_3A = (HK^{-1} - 4I)/4$ are full rank. It then follows that the columns of F_1 and and F_2 are linearly independent. Since no F_i matrix shares a column from the same $_jA$ matrix with any other F_k matrix, the columns of the F_i matrices are linearly independent.

C Rank of $GK^{-1} + 4I_{MN}$ and $HK^{-1} - 4I_{MN}$

We want to show that $GK^{-1} + 4I_{MN}$ is full rank. Note that,

$$GK^{-1} + 4I_{MN} = GK^{-1} + 4KK^{-1} = G(I_{MN} + 4K)K^{-1} \tag{167}$$

where I_{MN} is the $MN \times MN$ identity matrix. Since both G and K^{-1} are full rank, the only question is the rank of $(I_{MN} + 4K)$. Using the definitions,

$$G = I_M \otimes [D_N^s - I_N] \tag{168}$$
$$K = I_M \otimes Q_N + Q_M \otimes I_N, \tag{169}$$

we see that

$$
\begin{aligned}
(I_{MN} + 4K) &= (I_{MN} + 4I_M \otimes Q_N + 4Q_M \otimes I_N) \\
&= I_M \otimes I_N + 4I_M \otimes Q_N + 4Q_M \otimes I_N \\
&= \frac{1}{2}I_M \otimes I_N + 4I_M \otimes Q_N + 4Q_M \otimes I_N + \frac{1}{2}I_M \otimes I_N \\
&= \frac{1}{2}I_M \otimes (I_N + 8Q_N) + \frac{1}{2}(I_M + 8Q_M) \otimes I_N \\
&= I_M \otimes Q_{N1} + Q_{M1} \otimes I_N \\
&\triangleq K_1 \tag{170}
\end{aligned}
$$

35

where $Q_{M1} = \frac{1}{2}(I_M + 8Q_M)$ is an $M \times M$ tridiagonal, symmetric Toeplitz matrix,

$$Q_{M1} = \frac{1}{2} \begin{bmatrix} 5 & 1 & 0 & \dots & 0 \\ 1 & 5 & 1 & \ddots & \vdots \\ 0 & 1 & 5 & \ddots & 0 \\ \vdots & \ddots & \ddots & \ddots & 1 \\ 0 & \dots & 0 & 1 & 5 \end{bmatrix} \quad (M \times M) \tag{171}$$

Q_{N1} is similarily defined but has dimension $N \times N$. Q_{M1} can be readily seen to be full rank and can be diagonalized using the Ψ_M matrix. Q_{N1} can be readily seen to be full rank and can be diagonalized using the Ψ_N matrix.

For clarity, K_1 can be written as,

$$K_1 = \begin{bmatrix} Q_{N1} & 0 & 0 & \dots & 0 \\ 0 & Q_{N1} & 0 & \ddots & \vdots \\ 0 & 0 & Q_{N1} & \ddots & 0 \\ \vdots & \ddots & \ddots & \ddots & 0 \\ 0 & \dots & 0 & 0 & Q_{N1} \end{bmatrix} + \frac{1}{2} \begin{bmatrix} 5I_N & I_N & 0 & \dots & 0 \\ I_N & 5I_N & I_N & \ddots & \vdots \\ 0 & I_N & 5I_N & \ddots & 0 \\ \vdots & \ddots & \ddots & \ddots & I_N \\ 0 & \dots & 0 & I_N & 5I_N \end{bmatrix} \tag{172}$$

which can be written as,

$$K_1 = \frac{1}{2} \begin{bmatrix} Q_{N2} & I_N & 0 & \dots & 0 \\ I_N & Q_{N2} & I_N & \ddots & \vdots \\ 0 & I_N & Q_{N2} & \ddots & 0 \\ \vdots & \ddots & \ddots & \ddots & I_N \\ 0 & \dots & 0 & I_N & Q_{N2} \end{bmatrix} \tag{173}$$

where the $N \times N$ matrix Q_{N2} is defined,

$$Q_{N2} = \begin{bmatrix} 0 & 1 & 0 & \dots & 0 \\ 1 & 0 & 1 & \ddots & \vdots \\ 0 & 1 & 0 & \ddots & 0 \\ \vdots & \ddots & \ddots & \ddots & 1 \\ 0 & \dots & 0 & 1 & 0 \end{bmatrix} \quad (M \times M) \tag{174}$$

Some thought reveals that K_1 is full rank and therefore $GK^{-1} + 4I_{MN}$ is full rank. Using this same procedure it is easy to show that $HK^{-1} - 4I_{MN}$ is full rank.

D   Model Parmeter Extrapolation

From the results presented in Chapter 7 of [13] we can observe that initial values computed from dealiased point-wise wind estimates are generally of good quality if the wind speed

is sufficiently high. When a region contains contains an area of low wind speed, dealiasing errors may result in poor-quality initial values. Adjacent regions, however, are fine. With this in mind, the following question arises: once we have determined the model parameters for a given region, can we use this information to estimate the model parameters of an adjacent or overlapping region? While there are a number of ways to address this question, we will consider a particular technique which we have termed model extrpolation. In this approach, the model parameters determined for a given $M \times N$ region are extrapolated to an overlapping region where the overlap is $N - 1$ points in the N dimension (along-track). The extrapolated model parameter vector can then be used as an initial value for optimization of the model-based objective function for the new region.

D.1   Preliminaries

Before proceeding, we need to introduce some additional notation to simplify later development.

Let the elements $b_{i,j}^{ru}$ of the $M \times N$ matrix B^{ru} be defined, as

$$b_{i,j}^{ru} = \begin{cases} p_{i,N+1} & \text{if } 1 \leq i \leq M \text{ and } j = N \\ 0 & \text{otherwise.} \end{cases} \tag{175}$$

For clarity,

$$B^{ru} = \begin{bmatrix} 0 & \dots & 0 & p_{1,N+1} \\ \vdots & \ddots & \vdots & \vdots \\ 0 & \dots & 0 & p_{M,N+1} \end{bmatrix}. \tag{176}$$

Let $\overline{B}^{ru}$ be the lexicographic-ordered vector corresponding to B^{ru}.

In the PBC model, the pressure field boundary conditions in the vector $\overline{X}$ are parameterized using an M_l-order polynomial [see Eq. (105)] using the M_l element vector $\overline{Y}$ contain the coefficients of the boundary polynomial [see Eq. (107)]. Define the $MN \times M_l$ matrix Υ such that,

$$\overline{B} = \Upsilon \overline{Y}; \tag{177}$$

define the $MN \times M_l$ matrix Υ^u such that,

$$\overline{B}^u = \Upsilon^u \overline{Y}; \tag{178}$$

and define the $MN \times M_l$ matrix Υ^{ru} such that,

$$\overline{B}^{ru} = \Upsilon^{ru} \overline{Y}. \tag{179}$$

General expressions for Υ, Υ^u, and Υ^{ru} are complicated and so are not given here.

When the boundary conditions are not parameterized Eqs. (177) though (179) can still be used. In this case $M_l \triangleq 2M + 2N + 2$ and $\overline{Y}$ is replaced by $\overline{X}$.

D.2 Model Parameter Vector Extrapolation

Consider an $M \times N$ region $\mathcal{L}_1$ which overlaps a given $M \times N$ region $\mathcal{L}$ by $N-1$ points in the j index (along-track) and is aligned in the i index (cross-track). This corresponds to a region shifted just one sample in the j index (see Fig. 5). We will consider both $+1$ or -1 shifts. Essentially, we will be extrapolating the wind field along one edge just outside of the region $\mathcal{L}$ from the wind field within the region.

The boundary conditions are the pressure field along the outside edge of the region $\mathcal{L}$ boundary (see Fig. 1). The vector $\overline{B}^u$ contains the values of the pressure field at $(j=0, i=1, \ldots, N)$. If we examine the region $\mathcal{L}_1$ which is one sample in the $-j$ direction (see Fig. 5), we find that the boundary conditions in $\overline{B}^u$ contain the values of the pressure field at the new location $\mathcal{L}_1$. Further, the pressure field in $\mathcal{L}$ at $(i=M, j=1, \ldots, N)$ are the boundary conditions at the new location $\mathcal{L}_1$ included in the vector $\overline{B}^r$ for $\mathcal{L}_1$. The only new boundary conditions needed are at $(i=0, j=0)$, $(i=0, j=N+1)$, and $(i=-1, j=1, \ldots, N)$. These we can compute from the known pressure field values at the old location and the extropolated the vorticity and divergence fields at $(i=0, j=1, \ldots, N)$.

Let us start by assuming that we have the model parameter vector $\overline{X}$ at the starting region $\mathcal{L}$. Using the definition of $\overline{X}$ we can compute $\overline{B} = \overline{B}^u + \overline{B}^v + \overline{B}^r$, $\overline{C}$, and $\overline{D}$. The pressure field is computed using Eq. (35) (repeated here for clarity of presentation),

$$\overline{P} = \frac{1}{4} K^{-1} [\overline{B} + \overline{C}]. \tag{180}$$

Quantities for region $\mathcal{L}_1$ (the new location) will be identified by an underline while no underline indicates region $\mathcal{L}$ (the old location). The pressure field at the new location, $\underline{P}$, can be appropriately computed from B^u and P, i.e.,

$$\underline{P} = P T^T + B^u \tag{181}$$

where the $M \times N$ matrix T with elements $t_{i,j}$,

$$t_{i,j} = \begin{cases} 1, & \text{if } j \leq i \\ 0, & \text{otherwise.} \end{cases} \tag{182}$$

Using lexicographic vectors and matrix notation, Eq. (181) can be written, as

$$\underline{\overline{P}} = (I \otimes T)\overline{P} + \overline{B}^u \tag{183}$$

Note that, $I \otimes T = G + I_{MN}$.

The vorticity field at the new location $\mathcal{L}_1$, $\underline{\overline{C}}$, is computed by extrapolating the vorticity bivariate polynomial. Our model for the vorticity field $\zeta_{i,j}$ may be expressed as

$$\zeta_{i,j} = \sum_{\substack{m=0}}^{M_c} \sum_{\substack{n=0 \\ m+n \leq \max(M_c, N_c)}}^{N_c} c_{m,n} i^m j^n. \tag{184}$$

Let the number of parameters in the vorticity field model be N_v.
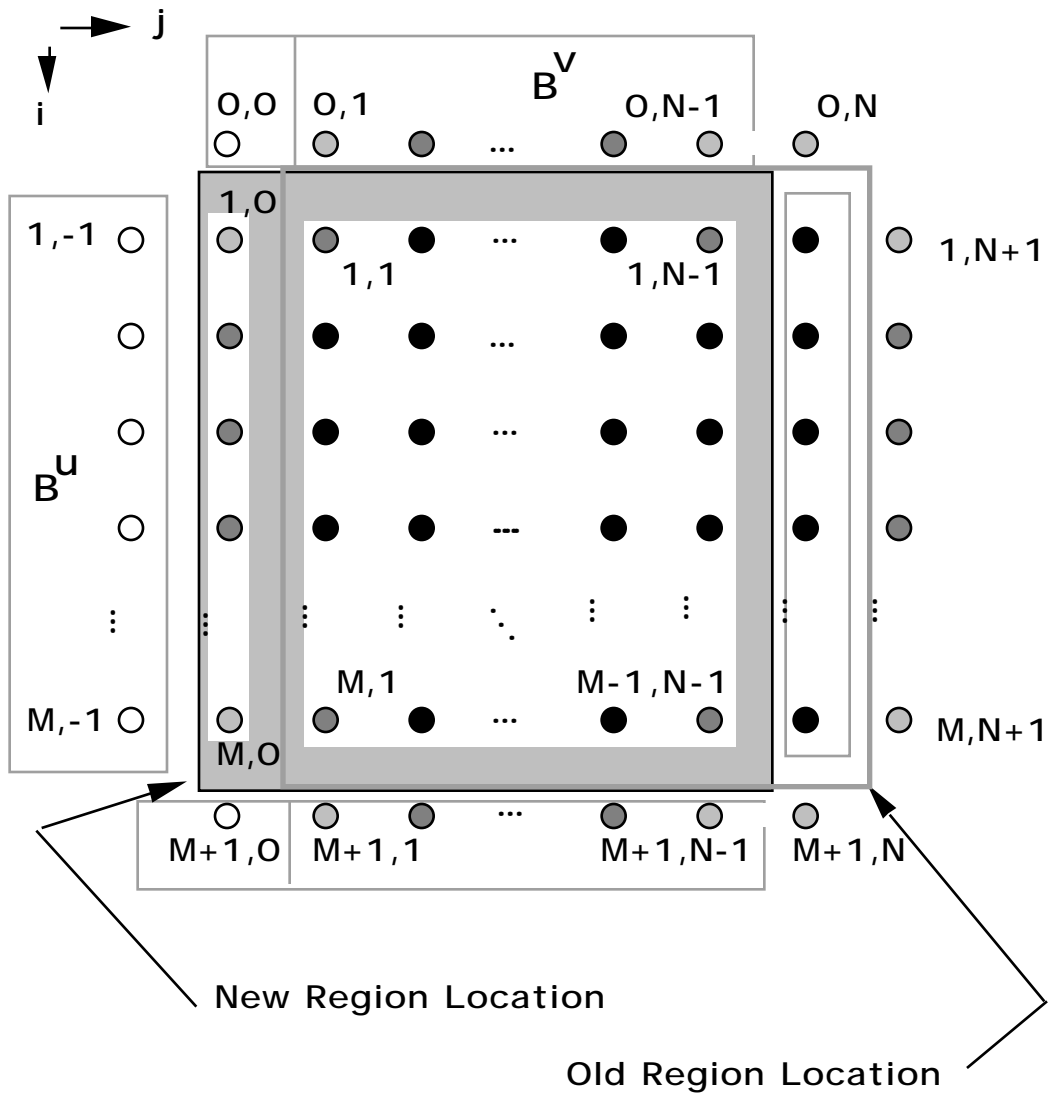
Figure 5: An illustration showing two $M \times N$ regions with $N-1$ overlap in the $-j$ direction. Note that the old B^u boundary conditions are now part of the pressure field in the region of interest. New boundary conditions needed are indicated with open circles (see text). Compare with Fig. 1

Table 10: Extrapolated vorticity coefficients for region $\mathcal{L}_1$ in terms of the vorticity coefficients for region $\mathcal{L}$

	$\overline{c_{m,n}}$ $\forall m$	
n	$(j-1)$ case	$(j+1)$ case
0	$c_{m,0} - c_{m,1} + c_{m,2} - c_{m,3} + c_{m,4}$	$c_{m,0} + c_{m,1} + c_{m,2} + c_{m,3} + c_{m,4}$
1	$c_{m,1} - 2c_{m,2} + 3c_{m,3} - 4c_{m,4}$	$c_{m,1} + 2c_{m,2} + 3c_{m,3} + 4c_{m,4}$
2	$c_{m,2} - 3c_{m,3} + 6c_{m,4}$	$c_{m,2} + 3c_{m,3} + 6c_{m,4}$
3	$c_{m,3} - 4c_{m,4}$	$c_{m,3} + 4c_{m,4}$
4	$c_{m,4}$	$c_{m,4}$

The vorticity field $\underline{\zeta_{i,j}}$ at the new location will be

$$\underline{\zeta_{i,j}} = \sum_{\substack{m=0 \\ }}^{M_c} \sum_{\substack{n=0 \\ m+n \leq \max(M_c, N_c)}}^{N_c} c_{m,n} i^m (j-1)^n \tag{185}$$

$$= \sum_{\substack{m=0 \\ }}^{M_c} \sum_{\substack{n=0 \\ m+n \leq \max(M_c, N_c)}}^{N_c} \underline{c_{m,n}} i^m j^n \tag{186}$$

Equating powers of j, $\underline{c_{m,n}}$ can be computed in terms of the coefficients $c_{m,n}$. Table 10 summaries the results for a given value of m. Results for both $j-1$ and $j+1$ are shown.

To obtain a matrix equation we note that the vorticity field $\overline{C}$ can be written, as

$$\overline{C} = \Upsilon^c \overline{X}^c \tag{187}$$

where Υ^c and $\overline{X}^c$ are defined in Eq. (86) ($\overline{X}^c$ contains the lexicographic-order vorticity field parameters $c_{m,n}$). The shifted and extrapolated vorticity field, $\overline{\underline{C}}$, can be written, as

$$\overline{\underline{C}} = \Upsilon^c \mathcal{T}_{-1}^c \overline{X}^c \tag{188}$$

where the $N_v \times N_v$ matrix $\mathcal{T}_{-1}^c$ contains the transformation of parameter values indicated above. Due to the complexity of a general definition of $\mathcal{T}_{-1}^c$, we give several numerical examples of $\mathcal{T}_{-1}^c$. For $M_c = N_c = 0$,

$$\mathcal{T}_{-1}^c = \begin{bmatrix} 1 \end{bmatrix}. \tag{189}$$

For $M_c = N_c = 1$,

$$\mathcal{T}_{-1}^c = \begin{bmatrix} 1 & -1 & 0 \\ 0 & 1 & 0 \\ 0 & 0 & 1 \end{bmatrix}. \tag{190}$$

For $M_c = N_c = 2$,

$$\mathcal{T}^c_{-1} = \begin{bmatrix} 1 & -1 & 0 & 1 & 0 & 0 \\ 0 & 1 & -1 & 0 & 0 & 0 \\ 0 & 0 & 1 & -2 & 0 & 0 \\ 0 & 0 & 0 & 1 & 0 & 0 \\ 0 & 0 & 0 & 0 & 1 & 0 \\ 0 & 0 & 0 & 0 & 0 & 1 \end{bmatrix}. \tag{191}$$

For shifts in the positive j direction, the signs of all the negative values in $\mathcal{T}^c_{-1}$ are changed to positive. For example, $\mathcal{T}^c_{+1}$, for $M_c = N_c = 3$ is,

$$\mathcal{T}^c_{+1} = \begin{bmatrix} 1 & 1 & 0 & 0 & 1 & 0 & 1 & 0 & 0 & 0 \\ 0 & 1 & 1 & 0 & 0 & 1 & 0 & 0 & 0 & 0 \\ 0 & 0 & 1 & 1 & 0 & 0 & 0 & 0 & 0 & 0 \\ 0 & 0 & 0 & 1 & 0 & 0 & 2 & 0 & 3 & 0 \\ 0 & 0 & 0 & 0 & 1 & 0 & 0 & 2 & 0 & 0 \\ 0 & 0 & 0 & 0 & 0 & 1 & 0 & 0 & 3 & 0 \\ 0 & 0 & 0 & 0 & 0 & 0 & 1 & 0 & 0 & 0 \\ 0 & 0 & 0 & 0 & 0 & 0 & 0 & 1 & 0 & 0 \\ 0 & 0 & 0 & 0 & 0 & 0 & 0 & 0 & 1 & 0 \\ 0 & 0 & 0 & 0 & 0 & 0 & 0 & 0 & 0 & 1 \end{bmatrix}. \tag{192}$$

The new vorticity field parameters $\underline{c_{m,n}}$ in $\underline{\overline{X}}^c$ can be expressed in terms of the old vorticity field parameters $c_{m,n}$ in $\overline{X}^c$, as

$$\underline{\overline{X}}^c = \mathcal{T}^c_{-1} \overline{X}^c. \tag{193}$$

Similarily, the new divergence field parameters $\underline{d_{m,n}}$ in $\underline{\overline{X}}^d$ can be expressed in terms of the old divergence field parameters $d_{m,n}$ in $\overline{X}^d$, as

$$\underline{\overline{X}}^d = \mathcal{T}^d_{-1} \overline{X}^d. \tag{194}$$

Having obtained the vorticity field $\overline{C}$ at the new location, we can compute the new boundary conditions. Note that we will compute all of the boundary conditions simultaneously from the new pressure field and extrapolated vorticity field. The new boundary condition vector $\underline{\overline{B}}$ is,

$$
\begin{aligned}
\underline{\overline{B}} &= 4K\underline{\overline{P}} - \underline{\overline{C}} \\
&= 4K[(I \otimes T)\overline{P} + \overline{B}^u] - \underline{\overline{C}} \\
&= K[(I \otimes T)K^{-1}(\overline{B} + \overline{C}) + 4\overline{B}^u] - \underline{\overline{C}}
\end{aligned} \tag{195}
$$

Let the $MN \times MN$ matrix $\mathcal{K}_{-1}$ be defined, as

$$\mathcal{K}_{-1} \triangleq K(I \otimes T)K^{-1}. \tag{196}$$

The boundary condition vector $\overline{B}$ is,

$$\overline{B} = \Upsilon \overline{Y}, \tag{197}$$

while the boundary condition vector $\overline{B}^u$ is, the $MN \times M_l$ matrix Υ^u for which

$$\overline{B}^u = \Upsilon^u \overline{Y}. \tag{198}$$

Note that a least-squares estimate of $\overline{Y}$ given $\overline{B}$ is,

$$\overline{Y} = \Upsilon^\dagger \overline{B} = (\Upsilon^T \Upsilon)^{-1} \Upsilon^T \overline{B} \tag{199}$$

where $\Upsilon^\dagger$ is the pseudo-inverse of Υ. Note that in the non-parameterized boundary condition case with $M = N$, $\Upsilon^\dagger$ will be full rank only when $M \geq 6$. Using Eq. (199), Eq. (195) can be written, as

$$\begin{aligned}
\underline{\overline{B}} &= \mathcal{K}_{-1}(\overline{B} + \overline{C}) + 4K\overline{B}^u - \underline{\overline{C}} \\
&= \mathcal{K}_{-1}(\Upsilon \overline{Y} + \Upsilon^c \overline{X}^c) + 4K\Upsilon^u \overline{Y} - \Upsilon^c \mathcal{T}_{-1}^c \overline{X}^c \\
&= \mathcal{K}_{-1}(\Upsilon + 4K\Upsilon^u)\overline{Y} + (\mathcal{K}_{-1}\Upsilon^c - \Upsilon^c \mathcal{T}_{-1}^c)\overline{X}^c.
\end{aligned} \tag{200}$$

The least-squares estimate of the shifted boundary parameters $\underline{\overline{Y}}$ is then,

$$\begin{aligned}
\underline{\overline{Y}} &= \Upsilon^\dagger \underline{\overline{B}} \\
&= \Upsilon^\dagger \left\{ \mathcal{K}_{-1}(\Upsilon + 4K\Upsilon^u)\overline{Y} + (\mathcal{K}_{-1}\Upsilon^c - \Upsilon^c \mathcal{T}_{-1}^c)\overline{X}^c \right\}.
\end{aligned} \tag{201}$$

Defining $\overline{X}^b$ as the concatenation of $\overline{Y}$, $\overline{X}^c$, and $\overline{X}^d$, i.e.,

$$\overline{X}^b = \left[\begin{array}{c} \overline{Y} \\ \hline \overline{X}^c \\ \hline \overline{X}^d \end{array} \right], \tag{202}$$

the new model parameter vector $\underline{\overline{X}}^b$ can be computed from the old parameter vector $\overline{X}^b$, as

$$\underline{\overline{X}}^b = M_{-1}\overline{X}^b \tag{203}$$

where the $N_p \times N_p$ matrix M_{-1} can be partioned as,

$$M_{-1} = \left[\begin{array}{c|c|c} M_{-1}^{bb} & M_{-1}^{bc} & 0 \\ \hline 0 & M_{-1}^{cc} & 0 \\ \hline 0 & 0 & M_{-1}^{dd} \end{array} \right] \tag{204}$$

where each of the partitions of M_{-1} are defined as follows: the $M_l \times M_l$ matrix M_{-1}^{bb} is,

$$M_{-1}^{bb} = \Upsilon^\dagger(\mathcal{K}_{-1}\Upsilon + 4K\Upsilon^u); \tag{205}$$

the $M_l \times N_c$ matrix M_{-1}^{bc} is,

$$M_{-1}^{bc} = \Upsilon^\dagger(\mathcal{K}_{-1}\Upsilon^c - \Upsilon^c \mathcal{T}_{-1}^c); \tag{206}$$

42

the $N_c \times N_c$ matrix M^{cc}_{-1} is,

$$M^{cc}_{-1} = \mathcal{T}^c_{-1}; \tag{207}$$

and the $N_d \times N_d$ matrix M^{dd}_{-1} is,

$$M^{dd}_{-1} = \mathcal{T}^d_{-1}. \tag{208}$$

The result is the model parameter vector extrapolated to the new region. This can be used to compute an initial value, which can be updated using the pointwise results for wind field estimation.

These results can be extended to motion in the $+j$ direction. For $+j$ movement, the boundary values which become part of the pressure field are at $(j = N+1, i = 1, \ldots, M)$ which are contained as part of the $\overline{B}^r$ vector, $\overline{B}^{ru}$. The derivation of the matrix to extrapolate the model parameter vector to the new location in the $+j$ direction is similar to the derivation for the $-j$ direction. The pressure field at the new location, $\underline{P}$, can be appropriately computed from B^{ru} and P, i.e.,

$$\underline{P} = PT + B^{ru} \tag{209}$$

(The difference between Eqs. (181) and (209) is the transpose on the T matrix.) Using lexicographic vectors and matrix notation, Eq. (209) can be written, as

$$\overline{P} = (I \otimes T^T)\overline{P} + \overline{B}^u \tag{210}$$

Note that, $I \otimes T^T = (G - I_{MN})^T$. The shifted and extrapolated vorticity field $\overline{C}$ is

$$\overline{C} = \Upsilon^c \mathcal{T}^c_{+1} \overline{X}^c \tag{211}$$

The new boundary condition vector $\overline{B}$ can be written, as

$$
\begin{aligned}
\overline{B} &= 4K\overline{P} - \overline{C} \\
&= 4K[(I \otimes T^T)\overline{P} + \overline{B}^{ru}] - \overline{C} \\
&= K[(I \otimes T^T)K^{-1}(\overline{B} + \overline{C}) + 4\overline{B}^{ru}] - \overline{C}
\end{aligned}
\tag{212}
$$

Let the $MN \times MN$ matrix $\mathcal{K}_{+1}$ be defined, as

$$\mathcal{K}_{+1} \triangleq K(I \otimes T^T)K^{-1}. \tag{213}$$

Noting that

$$\overline{B}^{ru} = \Upsilon^{ru}\overline{Y}, \tag{214}$$

a least-squares estimate of $\overline{Y}$ given $\overline{B}$ is,

$$\overline{Y} = \Upsilon^\dagger \overline{B} = (\Upsilon^T \Upsilon)^{+1} \Upsilon^T \overline{B} \tag{215}$$

where $\Upsilon^\dagger$ is the pseudo-inverse of Υ. Then Eq. (212) can be written, as

$$
\begin{aligned}
\overline{B} &= \mathcal{K}_{+1}(\overline{B} + \overline{C}) + 4K\overline{B}^{ru} - \overline{C} \\
&= \mathcal{K}_{+1}(\Upsilon \overline{Y} + \Upsilon^c \overline{X}^c) + 4K\Upsilon^{ru}\overline{Y} - \Upsilon^c \mathcal{T}^c_{+1} \overline{X}^c \\
&= \mathcal{K}_{+1}(\Upsilon + 4K\Upsilon^{ru})\overline{Y} + (\mathcal{K}_{+1}\Upsilon^c - \Upsilon^c \mathcal{T}^c_{+1})\overline{X}^c.
\end{aligned}
\tag{216}
$$

43

The least-squares estimate of the shifted boundary parameters $\underline{\overline{Y}}$ is then,

$$
\begin{aligned}
\underline{\overline{Y}} &= \Upsilon^\dagger \underline{\overline{B}} \\
&= \Upsilon^\dagger \left\{ \mathcal{K}_{+1}(\Upsilon + 4K\Upsilon^{ru})\overline{Y} + (\mathcal{K}_{+1}\Upsilon^c - \Upsilon^c \mathcal{T}_{+1}^c)\overline{X}^c \right\}.
\end{aligned}
\tag{217}
$$

Then the new model parameter vector $\underline{\overline{X}}^b$ can be computed from the old parameter vector $\overline{X}^b$, as

$$
\underline{\overline{X}}^b = M_{+1}\overline{X}^b
\tag{218}
$$

where the $N_p \times N_p$ matrix M_{+1} can be partioned as,

$$
M_{+1} = \left[
\begin{array}{c|c|c}
M_{+1}^{bb} & M_{+1}^{bc} & 0 \\
\hline
0 & M_{+1}^{cc} & 0 \\
\hline
0 & 0 & M_{+1}^{dd}
\end{array}
\right]
\tag{219}
$$

where each of the partions of M_{+1} are defined as follows: the $M_l \times M_l$ matrix M_{+1}^{bb} is,

$$
M_{+1}^{bb} = \Upsilon^\dagger(\mathcal{K}\Upsilon + 4K\Upsilon^{ru});
\tag{220}
$$

the $M_l \times N_c$ matrix M_{+1}^{bc} is,

$$
M_{+1}^{bc} = \Upsilon^\dagger(\mathcal{K}\Upsilon^c - \Upsilon^c \mathcal{T}_{+1}^c);
\tag{221}
$$

the $N_c \times N_c$ matrix M_{+1}^{cc} is,

$$
M_{+1}^{cc} = \mathcal{T}_{+1}^c;
\tag{222}
$$

and the $N_d \times N_d$ matrix M_{+1}^{dd} is,

$$
M_{+1}^{dd} = \mathcal{T}_{+1}^d.
\tag{223}
$$

The result is the model parameter vector extrapolated to the new region in the positive j direction.

D.3   Discussion

The matrix M_{-1} (or M_{+1}) gives us a very simple way of "predicting" (by extrapolation) what the model parameter vector for an $N-1$ overlapped region (in the $-j$ or $+j$ direction) will be from the model parameters of a given region. Using the point-wise wind estimation and dealiasing procedure described in Chapter 6, we can first select a region which has a high wind speed using the average wind speeds from the point-wise ambiguity sets. For high wind speed regions, the dealiased wind fields provide good initial values. Given an initial wind field, we compute the initial model parameters and optimize the field-wise objective function. Using the model extrapolation technique described here we can use M_{-1} (M_{+1}) to predict the model parameters for an adjoining region containing a large area of low wind speeds. This approach can give better initial values than the point-wise dealiasing approach.

As with any extrapolation, one must apply the model extrapolation approach with great care. This is especially true in regions where the wind field model does not fit the

underlying wind field well. Improved performance for the model extrapolation approach can be obtained by first computing the extrapolated model parameter vector, computing the resulting wind field, and then, for each sample point, selecting the ambiguity from the point-wise wind estimate set which is closest to the predicted wind field. The initial value is then computed from this closest ambiguity field. The model vector is then optimized and the process repeated with the region sliding along the measurement swath to cover the low wind speed area.

References

[1] R. Beven and M. Freilich, "Wind Fields for Big Sim," Jet Propulsion Laboratory Interoffice Memorandum, Nov. 1985.

[2] S. J. Bijlsma, L. M. Hafkenscheid and P. Lynch, "Computation of the Streamfunction and Velocity Potential and Reconstruction of the Wind Field," *Monthly Weather Review*, No. 114, pp. 1547-1551, 1986.

[3] J. W. Brewer, "Kronecker Products and Matrix Calculus in System Theory," *IEEE Transactions on Circuits and Systems*, Vol. CAS-25, No. 9, pp. 772-781, Sept. 1978.

[4] R. A. Brown *et al.*, "Surface Wind Analyses for SEASAT," *Journal of Geophysical Research*, Vol. 87, No. C5, pp. 3355-3364, April 1982.

[5] C. J. Cats, "Analysis of Surface Wind and Its Gradient in a Mesoscale Wind Observation Network," *Monthly Weather Review*, Vol. 108, pp. 1100-1107, Aug. 1980.

[6] M. H. Freilich and D. B. Chelton, "Wavenumber Spectra of Pacific Winds Measured by the Seasat Scatterometer," *Journal of Physical Oceanography*, Vol. 16, No. 4, pp. 741-757, April 1986.

[7] H. F. Hawkins and S. L. Rosenthal, "On the Computation of Stream Functions from the Wind Field," *Monthly Weather Review*, Vol. 93, pp. 245-253, April 1965.

[8] A. K. Jain and J. R. Jain, "Partial Differential Equations and Finite Difference Methods in Image Processing–Part II: Image Restoration," *IEEE Transactions on Automatic Control*, Vol. AC-23, No. 5, pp. 817-834, Oct. 1978.

[9] S. J. Leon, *Linear Algebra with Applications*, New York: MacMillan Pub. Co., Inc., 1980.

[10] F. Li, P. Callahan, M. Freilich, D. Long, and C. Winn, "NASA Scatterometer for NROSS – A System for Global Oceanic Wind Measurement," Proceedings of the International Geoscience and Remote Sensing Symposium, pp. 777-780, 1984.

[11] F. Li, C. Winn, D. Long, and C. Guey, "NROSS Scatterometer – An Instrument for Global Oceanic Wind Observations," Proceedings of SPIE – The International Society for Optical Engineering, Vol. 481, pp. 193-198, 1984.

[12] D. G. Long and J. M. Mendel, "Model-based Estimation of Wind Fields Over the Ocean from Wind Scatterometer Measurements," Proceeding of the International Geoscience and Remote Sensing Symposium, pp. 553-556, 1988.

[13] D. G. Long, "Model-based Estimation of Wind Fields Over the Ocean from Wind Scatterometer Measurements," Ph.D. Dissertation, University of Southern California, 1989.

[14] P. Lynch, "Deducing the Wind from Vorticity and Divergence," *Monthly Weather Review*, Vol. 116, pp. 86-93, Jan. 1988.

[15] P. Lynch, "Partioning the Wind in a Limited Domain," *Monthly Weather Review*, Vol. 117, pp. 1492-1500, July 1989.

[16] R. A. Maddox and T. H. Vonder Haar, "Covariance Analyses of Satellite-Derived Mesoscale Wind Fields," *Journal of Applied Meteorology*, Vol. 18, pp. 1327-1334, Oct. 1979.

[17] A. R. Mitchell, *Computational Methods in Partial Differential Equations*, London: John Wiley and Sons, 1969.

[18] S. V. Parter, "Remarks on the Numerical Computation of Solutions of $\Delta u = f(P, u)$," *Numerical Solution of Partial Differential Equations*, J. H. Bramble, ed., New York: Academic Press, pp. 73-82, 1966.

[19] W. J. Pierson, Jr., "The Measurement of the Synoptic Scale Wind Over the Ocean," *Journal of Geophysical Research*, Vol. 88, No. C3, pp. 1683-1708, Feb. 1983.

[20] W. J. Pierson, Jr., W. B. Sylvester, and R. E. Salfi, "Vector Wind, Horizontal Divergence, Wind Stress, and Wind Stress Curl from SEASAT-SASS at a One Degree Resolution," NASA Conference Publication 2303, Proceedings of the URSI Commision F Symposium and Workshop, Shoresh, Israel, pp. 557-565, May 14-23, 1984.

[21] M. M. Rienecker and L. L. Ehret, "Wind Stress Curl Variability Over the North Pacific from the Comprehensive Ocean-Atmosphere Data Set," *Journal of Geophysical Research*, Vol. 93, No. C5, pp. 5069-5077, May 1988.

[22] J. Shukla and K. R. Saha, "Computation of Non-Divergent Streamfunction and Irrotational Velocity Potential from the Observed Winds," *Monthly Weather Review*, Vol. 102, pp. 419-425, June 1974.

[23] J. Willebrand, "Temporal and Spatial Scales of the Wind Field over the North Pacific and North Atlantic," *Journal of Physical Oceanography*, Vol. 8, pp. 1080-1094, 1978.

[24] T-W Yu, "A Technique for Deducing Wind Direction from Satellite Microwave Measurements of Wind Speed," *Monthly Weather Review*, Vol. 115, pp. 1929-1939, Sept. 1987.